

REPUBLIQUE ALGERIENNE DEMOCRATIQUE ET POPULAIRE  
MINISTERE DE L'ENSEIGNEMENT SUPERIEUR  
ET DE LA RECHERCHESCIENTIFIQUE

UNIVERSITE DES FRERES MENTOURI CONSTANTINE 1  
FACULTE DES SCIENCES EXACTES  
DEPARTEMENT DE PHYSIQUE

N° d'ordre: .....

Série: .....

**THESE**

POUR OBTENIR LE DIPLOME DE DOCTORAT  
3<sup>ème</sup> CYCLE (LMD) EN PHYSIQUE  
Spécialisté: PHYSIQUE THEORIQUE

**THEME:**

---

DEVELOPPEMENT MATHEMATIQUE ET APPLICATIONS DE  
LA GRAVITATION QUANTIQUE A BOUCLES

---

Presentée par:

**AHMIDA BENDJOUDI**

Soutenue le:.../.../2016

Devant le jury

**Président:**

Mr. K. Ait Moussa      Prof.      Université des frères Mentouri Constantine 1

**Rapporteur:**

Mr. N. Mebarki      Prof.      Université des frères Mentouri Constantine 1

**Examineurs:**

Mr. H. Aissaoui      Prof.      Université des frères Mentouri Constantine 1

Mr. A. Bouchared      M.C.A.      Université Badji Mokhtar, Annaba

# *Acknowledgements*

My gratitude for five years of friendship, clear thinking and fun to explore and learn together: To my supervisor Nouredine Mebarki and my fellow students. Vivid discussions have nourished my work. Special thanks to my supervisor (for improving my English), to K. Ait Moussa, H. Aissaoui and A. Bouchared.

Foremost, I thank my family, my parents to whom I dedicate this thesis.

# Contents

<b>Acknowledgements</b>	<b>i</b>
<b>Contents</b>	<b>ii</b>
<b>List of Figures</b>	<b>v</b>
<b>List of Tables</b>	<b>vii</b>
<b>1 Introduction</b>	<b>1</b>
<b>2 Loop gravity</b>	<b>5</b>
2.1 The Group of Loops . . . . .	6
2.2 Infinitesimal Generators of the Group of Loops . . . . .	6
2.2.1 Loop Algebra . . . . .	7
2.3 Loop structure . . . . .	8
2.4 Spin Network States . . . . .	9
2.4.1 Dynamics . . . . .	9
<b>3 Spinfoam</b>	<b>12</b>
3.1 3 dimensional Euclidean gravity . . . . .	12
3.1.1 Kinematical Hilbert space . . . . .	12
3.1.2 Invariance . . . . .	13
3.1.3 Basis . . . . .	13
3.1.4 Dynamics . . . . .	14
3.2 4 dimensional Lorentzian gravity . . . . .	15
3.2.1 Discretization . . . . .	15
3.2.2 Variables . . . . .	15
3.2.3 States . . . . .	16
3.2.4 Transition amplitudes . . . . .	17
<b>4 Length of Space Quantization</b>	<b>18</b>
4.1 Bianchi's quantization of the length of space . . . . .	18
4.1.1 Construction of the length operator . . . . .	19
4.1.2 Tikhonov Regularization . . . . .	19

4.1.3	External Regularization: the Two-Hand Operator . . . . .	20
4.2	Thiemann’s quantization of the length of space . . . . .	21
4.2.1	Regularization . . . . .	21
4.2.2	The Spectrum . . . . .	22
4.3	Ma’s quantization of the length of space . . . . .	23
4.4	Semiclassical Quantization of the Length of Space . . . . .	24
4.4.1	Tetrahedra Space of Shapes . . . . .	24
4.4.2	The Length of Space Quantization . . . . .	25
4.4.2.1	The volume of space quantization . . . . .	25
4.4.2.2	The angle of space quantization . . . . .	26
4.4.2.3	The length of space quantization . . . . .	27
<b>5</b>	<b>The quantum polyhedra</b> . . . . .	<b>29</b>
5.1	The phase space of polyhedra . . . . .	29
5.2	Polyhedra from areas and normals . . . . .	31
5.3	Relation to loop quantum gravity . . . . .	31
5.4	The quantum tetrahedron . . . . .	31
5.5	Bohr-Sommerfeld quantization . . . . .	32
5.5.1	Old quantum theory . . . . .	32
5.5.2	Heisenberg Representation . . . . .	33
5.5.2.1	Mathematical derivation . . . . .	33
5.5.2.2	Matrix mechanics . . . . .	34
5.5.3	Canonical commutation relations . . . . .	36
5.5.3.1	Transformation theory . . . . .	36
5.5.4	Symmetry . . . . .	37
5.6	The Quantum Trihedron . . . . .	37
5.6.1	The Areas and Volume of Tetrahedron as Boundaries and Bulk . . . . .	38
5.6.2	The Quantization . . . . .	39
5.6.3	The first strategy . . . . .	39
5.6.4	The second strategy . . . . .	43
5.7	The quantum Trihedron: Generalization . . . . .	44
<b>6</b>	<b>The Complete Spectrum of the Volume of Space from Bohr-Sommerfeld Quantization</b> . . . . .	<b>46</b>
6.1	The Quantum Polyhedron: The volume Spectrum . . . . .	46
6.2	Examples . . . . .	48
6.2.1	The three valent node $\mathcal{H}_3$ : trihedron . . . . .	48
6.2.2	The four valent node $\mathcal{H}_4$ : tetrahedron . . . . .	48
6.2.3	The five valent node $\mathcal{H}_5$ : pentahedron . . . . .	49
6.2.3.1	The chaotic behavior . . . . .	50
<b>7</b>	<b>The Quantum Pentahedra</b> . . . . .	<b>51</b>
7.1	The Haggard’s Rescaling Reconstruction . . . . .	51
7.2	An alternative approach to the pentahedron volume . . . . .	52

---

7.3	The physical interpretation . . . . .	54
<b>8</b>	<b>Regge and Twisted Geometries in Loop Gravity</b>	<b>56</b>
8.1	Regge and twisted geometries . . . . .	56
8.2	Twisted Geometries from Holonomy-Flux variables computation . .	58
<b>9</b>	<b>Regge and Twisted Geometries in Schwarzschild Spacetime</b>	<b>62</b>
9.1	The quantum Schwarzschild spacetime . . . . .	62
<b>10</b>	<b>Space Density from Loop gravity</b>	<b>67</b>
10.1	Space Density . . . . .	67
10.2	Gravity as Mass Defect . . . . .	70
10.2.1	Gravity Force . . . . .	72
10.2.2	Gravitational Potential Energy . . . . .	72
<b>11</b>	<b>Conclusion</b>	<b>74</b>
11.1	Summary of the Key Results . . . . .	74
11.2	Future Research Interests . . . . .	75
<b>A</b>	<b>The <math>SL(2, C)</math> representations</b>	<b>77</b>
	<b>Bibliography</b>	<b>79</b>
	<b>Résumé</b>	<b>87</b>
	<b>Abstract</b>	<b>88</b>

# List of Figures

2.1	Spin network graph the corresponding dual picture . . . . .	10
5.1	Polyhedron with $N$ faces . . . . .	30
5.2	A parametrized tetrahedron $\tau(\sigma)$ at the minimum value of its volume (with respect to the variation in $\sigma$ ) in spectrum, such that $\sigma$ is defined in the neighborhood of $\lambda = 0$ . . . . .	38
5.3	A symplectic line encircled (bounded) by two phase space points. The length of this line is $2\pi(n + \frac{1}{2})$ times the Planck constant, where (for this case) $n = 2$ . . . . .	43
6.1	The network dual to polyhedra faces. . . . .	47
6.2	The Lorenz attractor displays chaotic behavior. These two plots demonstrate sensitive dependence on initial conditions within the region of phase space occupied by the attractor. . . . .	50
7.1	The P's graph as two connected tetrahedral graphs, which are dual to two connected tetrahedra $T_1$ and $T_2$ by the area $ \vec{A}_3 $ dual to $j_3$ .	53
7.2	The quantum tetrahedron depicted on phase spaces. Its areas are presented by points-like particles moving on the corresponding phase-space-orbits. The big black point refer to the area $ \vec{A}  =  \vec{A}_1 + \vec{A}_2  =  \vec{A}_3 + \vec{A}_4 $ , which represents, in turn, a point-like particle playing the role of the tetrahedron's noyau. . . . .	54
7.3	(a) Two connected tetrahedra by the area $ \vec{A}_3 $ . The illustration is intended to be considered to imagine the real case (orbits in 3d space). (b) The two tetrahedral noyaux of $T_1$ and $T_2$ moving on the corresponding phase-space-orbits around a common center called the pentahedron's noyau. The big blue point refer to the area $ \vec{A}_P $ of P defined by $ \vec{A}_P  =  \vec{A}_1 + \vec{A}_2 + \vec{A}_3  =  \vec{A}_4 + \vec{A}_5 + \vec{A}_3 $ , which is playing the role of the pentahedron's noyau moving long the corresponding phase-space-orbits of the pentahedron. . . . .	55
8.1	Two connected tetrahedra by an area with no matching in the area-configuration. The two points $p_1$ and $p_2$ refer to the general location inside the tetrahedra (not single points) . . . . .	59

---

9.1	A source of gravity (the big ball) and test particle (the small ball) embedded in a 2d graph. The illustration is intended to be considered to imagine the real case which is in three dimensional space: each triangle is replaced by a tetrahedron and the 2d graph becomes 3d one. The dashed lines refer to the presence of additional structures not presented. . . . .	65
10.1	Three tetrahedra with a common corner. This illustrates the real case (three dimensional space); the triangles are replaced by tetrahedra and the 2d areas becomes 3d regions. . . . .	67
10.2	(a) $n$ tetrahedra with a common corner. This illustrates the real case (three dimensional space); the triangles are replaced by tetrahedra and the 2d areas becomes 3d regions. (b) A visualization to the space density, around the gravity source, using color intensity. (c) A continuous approximation (analytic) to the space density as a function of $\rho$ . The dashed line in (a) refers to additional structures which are not presented here. . . . .	69

# List of Tables

4.1	Comparison of the Bohr-Sommerfeld and loop gravity length spectrum. The tetrahedral areas are assumed quantized equidistantly via $A_i = j_i + \frac{1}{2}, i = \overline{1,4}$ . The tetrahedral volume used in computing the length spectrum was computed separately for both the semiclassical and canonical derivation. . . . .	27
5.1	Comparison between the Bohr-Sommerfeld (BS) and loop gravity (LG) area spectrum. The accuracy values are computed as $accuracy = \frac{(BS-LG)*100}{BS}$ . . . . .	45



# Chapter 1

## Introduction

During the last years, a remarkable interest to loop quantum gravity has been devoted [1–4]. The discreteness of space quantities (area, volume, length and angle) has been the most fundamental result of the theory [5–16]. The main virtue of the theory lies in the fact that it starts from general theory of relativity via canonical, covariant [17–26] and geometrical [27–35] approaches to end up with same results.

The canonical approach was the first step in developing this new quantum theory of gravity. Within it, several works have been developed starting from the Ashtekar paper of Ref. [36] with imaginary connection (later, the connection was modified to be real variant, see for instant Refs. [37, 38]) which led to the solution of Wheeler-DeWitt equation [39] as Wilson loops. This had been the fertile ground for Rovelli and Smolin to find the loops representation [40]. The theory then has become well defined especially after introducing  $d_0$  measure (which is diffeomorphism invariant) by Ashtekar and al. [41, 42]. This construction led immediately to the expected results which are the discreteness of area and volume [43]. Despite all of these developments, the Hamiltonian constraints still having difficulties until the papers by Thiemann of Refs. [44–46]. In the practical dealing point of view, the theory (via the framework of Ref. [47]) reproduces the entropy of black holes, see for instance Ref. [48].

In the covariant approach, several models have been assumed starting from the model by Barrett–Crane of Ref. [49], that has been further motivated by Baez in Ref. [50]. In fact, this model was the expected result after the paper by Barbieri of Ref. [51] and its generalization demonstrated in Ref. [52]. The most well-known

model is that by The Engle–Pereira–Rovelli–Livine (EPRL) in which the basic idea has been that one has to relax the imposition of the Plebanski constraints that reduce BF theory to general relativity (imposing the constraints weakly). Another model which reproduces the results of the above model in some limits has been given by Freidel–Krasnov (FK) in Ref. [53]. In the latter, the coherent state representation has been used as a main technical tool. Other models have been explored and introduced. I refer, for a detailed overview on these models, to Ref. [54].

In the geometric approach, the research started considerably with the paper by Bianchi and et. al. -polyhedron in loop gravity- of Ref. [27]. A remarkable paper which motivated the search very much in the field of the quantum Polyhedra has been the one by Bianchi and Hall Haggard of Ref. [28] on the discreteness of the volume of space in which the authors provide an explicit semi-classically computation of the volume of space. The authors showed a remarkable compatibility, in the results, with the canonical derivation of the spectrum of the volume of space studied in Ref. [11].

This thesis is organized as follows:

- In chapter 2, we summarize the fundamental structure of the theory in a quick brief overview in which we fix the notation and the reader makes himself familiar with the notions and definitions. We start by investigating the main problems and their solutions by the loops representations (according to the paper by Rovelli and Smolin). We give in addition a simple description about the loop algebra in order that the mathematical part of the theory gets an easy access for the reader.
- In chapter 3, the covariant formulation of the theory is explored and studied in an easy way close to the usual language considered often in the loop gravity lectures. We take the two cases: (a) the three Euclidean dimensional quantum gravity in which we compute the amplitude and give the variables that reproduce it; (b) we also study the four dimensional case and the corresponding amplitude. This chapter is not explored in enough details in order to be readable for a beginner reader. We refer to Refs. [1, 2] for more details in which the authors provide a complete derivation in an easy way and accessible for all.

- In chapter 4, the length of space quantization is addressed. We summarize the current searches on the field in the context of the three papers of Refs. [55–57]. The semi-classical study of the length of space quantization has not been considered in the literature yet (up the work done by us of Ref. [58]), we therefore demonstrate our contribution on the field. In this contribution, we compare the results obtained by us with those found canonically.
- In chapter 5, the quantum Polyhedra is investigated. We give an introductory overview to the field and its relation with loop gravity. As our quantization is rather semi-classical based essentially on the arguments by Bohr and Sommerfeld (Bohr Sommerfeld quantization condition), we give an overview about the old quantum theory in order that the thesis be self-contained as much as possible. Then, we describe our contribution in the field, the quantum trihedron shown in Refs. [59, 60] and its generalization.
- In chapter 6, we give a generalization to the work done in Ref. [27] which has been explored in Ref. [61]. The study aims at completing the derivation of the discreteness of the volume of space and its spectrum for any node Hilbert with arbitrary valency.
- In chapter 7, we study the quantum pentahedron [62], a new proposed model for the quantum pentahedral volume. We give a nice representation for the atoms of space (tetrahedron and pentahedron). The volume spectrum proposed for the quantum polyhedron is compared with the one found by Hall Haggard.
- In chapter 8, we investigate the generalization [63] of the work done by Rovelli and et al. to the case of twisted truncation of general relativity. In Rovelli’s paper, the truncation is supposed to be the Regge one, our truncation is taken more generally, twisted truncation, where graphs present polyhedral structure in which the areas connecting tetrahedra do not define the same configuration.
- In chapter 9, we address the discretization of the Schwarzschild spacetime graph [64]. The method adopted in this work is the idea, concluded in loop gravity, that the areas variables are the natural variables in describing the structure of spacetime. The results found open new trends in studying the quantum spacetime according to the concluded general visualization about the gravity effects on a test particle.

- 
- The results obtained in chapter 9 lead to introduce a new quantity, in chapter 10, called space density [65]. This quantity plays the same role as the one in the usual density known in ordinary matter. This new quantity leads to new avenues since the results already understood in ordinary matter can be explored and studied to discover new properties about the spacetime structure.

# Chapter 2

## Loop gravity

The starting point in the canonical construction (or generally, in loop gravity) is general relativity formulated in terms of sen-Ashtekar-Barbaro connection [66, 67] in which  $SU(2)$  connections  $A_a^i(x)$  can be complex or real. In literature, the real connection approach is more used because of its simplicity.

Let us consider a three dimensional initial hypersurface data manifold  $M$  without boundaries, the  $SU(2)$  connections  $A_a^i(x)$  and the vector density  $E_a^i(x)$ . The indices  $i, j, \dots$  refer to locality and  $a, b, \dots$  to the general curved spatial coordinates  $x$ . The quantities  $E_a^i(x)$  are related to the metric of space via  $gg^{ab} = E_i^a E_i^b$  where  $g = \det g_{ab}$  and

$$A_a^i(x) = \Gamma_a^i(x) + \gamma k_a^i(x) \quad (2.1)$$

such that the triads  $\{e_b^i(x)\}$  satisfy  $\partial_{[a} e_{b]}^i(x) = \Gamma_{[a}^i(x) e_{b]j}(x)$ . The quantities  $\Gamma_a^i(x)$  and  $k_a^i(x)$  called spin connection and extrinsic curvature respectively. The quantity  $\gamma$  called Immirzi parameter. Picking up a value for it amounts to pick up a model, e.g. the choice  $\gamma = 1$  corresponds to Euclidean Hamiltonian constraints and  $\gamma = \sqrt{-1}$  corresponds to the Lorentzian Hamiltonian constraints. However, this constant has been fixed in order that the Bekenstein-Hawking formula is reproduced [68, 69].

## 2.1 The Group of Loops

Let  $M$  be a manifold, in which we consider the embedded piecewise smooth and continuous curve  $p$  defined via the map

$$p : [0, s_1] \cup [s_1, s_2] \dots [s_{n-1}, 1] \rightarrow M. \quad (2.2)$$

The composition of two curves  $p_1$  and  $p_2$  can be symbolized as  $p_1 o p_2$ . The inverse of a curve  $p$  is symbolized via  $p^{-1}(s) := p(1 - s)$ . The strategy in doing so is that (as convention) the interval is always has to be defined in a length of interval that equals to the unity. Let us now consider a closed curve  $L_0$  and the lie algebra-valued one form  $A_a$  on  $M$ . The parallel transport along  $L_0$  is given by a quantity called holonomy which takes the definition

$$H_A(l) = \mathcal{P} \exp \left\{ \int_l A_a(y) dy^a \right\}. \quad (2.3)$$

This holonomy has some properties:

1. it takes the simple definition:  $\hat{l}(1) = H_A(l)\hat{l}(0)$ ; where the hat  $\hat{\phantom{x}}$  refers to lifting the curve  $L_0$  to the principle fiber bundle  $P(M, G)$  of the group  $G$ ;
2. it is defined as the product of holonomies once we have successive curves composition. For the case of two curves  $l_1$  and  $l_2$  we have:  $H_A(l_1 o l_2) = H_A(l_1)H_A(l_2)$
3. it transforms once the points at which the curves get closed (on  $P(M, G)$ ) transform by a group element  $g$  of  $G$  via the relation:  $\acute{H}_A(l) = g^{-1}H_A(l)g$ .

## 2.2 Infinitesimal Generators of the Group of Loops

We denote by  $\mathcal{L}_0$  the set of loops with the composition operation  $o$ . Let us first talk a little about the notion of continuity, which can be defined for  $\mathcal{L}_0$  as follows: for any two loops  $\alpha$  and  $\beta$  we guaranty that these loops are closed iff there are two curves  $a \in \alpha$  and  $b \in \beta$  such that  $a$  belongs to the neighbor  $U_\epsilon(\beta)$  of  $\beta$ . The notion of continuity leads naturally to the notion of derivative or loop derivative. This leads to the notion of the infinitesimal change in performing the parallel transport along a loop  $\gamma$  once this loop is deformed by an infinitesimal loop  $\delta\gamma$ .

The infinitesimal loop introduced here is defined via the map  $\pi_o^x$  where  $o$  refers to the base-point of  $\gamma$  and  $x$  refers to the base-point of  $\delta\gamma$ . It encircles, in addition, an infinitesimal area defined by two unit vectors  $u$  and  $v$ . We suppose that we have functions  $\Psi(\delta\gamma, \gamma, \pi_o^x)$  depend on these infinitesimal variations. We attempt to study the Taylor expansion of them. It is natural that for the case of two dimensional perturbation, the first term is given by a derivative of the two dimensional expanded functions multiplied with two differential form. This can be given via

$$\Psi(\delta\gamma, \gamma, \pi_o^x) = \left(1 + \frac{1}{2}\sigma^{ab}\Delta_{ab}\right) \Psi(\delta\gamma, \gamma, \pi_o^x)|_{o\approx x} \quad (2.4)$$

such that  $\sigma^{ab} = 2\epsilon_1\epsilon_2(u^{[a}v^{b]})$  where  $\epsilon_1$  and  $\epsilon_2$  are the infinitesimal displacement towards  $u$  and  $v$  respectively. The quantity  $\Delta_{ab}$  called the derivative of the loop  $\gamma$ . Furthermore, one can go further and compute the second derivative which takes the form of a commutator of two areas elements, that is

$$\Psi(\delta\gamma_1, \delta\gamma_2, \gamma) = \left(1 + \frac{1}{4}\sigma_1^{ab}\sigma_2^{cd}[\Delta_{ab}(\pi_o^x), \Delta_{cd}(\pi_o^y)]\right) \Psi(\delta\gamma_1, \delta\gamma_2, \gamma)|_{o\approx(x,y)} \quad (2.5)$$

### 2.2.1 Loop Algebra

Let us consider a loop  $\alpha$  in which we set  $n$  points  $s_1, s_2, s_3, \dots, s_n \in \alpha$ . The parallel transport along  $\alpha$  called holonomy which is symbolized as  $U_\alpha$  and can be defined via

$$\mathcal{T}[\alpha] = -\text{Tr}[U_\alpha], \quad (2.6)$$

$$\mathcal{T}^a[\alpha](s) = -\text{Tr}[U_\alpha(s, s)E^a(s)]. \quad (2.7)$$

For the partition with  $n$  points, the algebra read

$$\mathcal{T}^{a_1 \dots a_n}[\alpha](s_1, \dots, s_n) = -\text{Tr}[U_\alpha(s_1, s_n)E^{a_n}(s_n)U_\alpha(s_1, s_n) \dots E^{a_1}(s_1)]. \quad (2.8)$$

where  $E^{a_n}(s_n) = -iE_i^a(x)\sigma_i$  and  $\{\sigma_i\}$  are the Pauli matrices. The holonomy  $U_\alpha$  has to satisfy the differential equation:

$$U_\alpha(1, s) = \frac{d\alpha_a(s)}{ds} A_a(\alpha(s)) U_\alpha(1, s) \quad (2.9)$$

where  $A_a = -\frac{i}{2}A_a^i(x)\sigma_i$ , that is

$$U_\alpha(s_1, s_2) = \mathcal{P} \exp \left\{ \int_{s_1}^{s_2} A_a(\alpha(s)) ds \right\}. \quad (2.10)$$

These called loop observables. Their phase space known phrased as the loop algebra. Moreover, one can compute the the Poisson brackets between  $\mathcal{T}[\alpha]$  and  $\mathcal{T}^a[\alpha](s)$  and get:

$$\{\mathcal{T}[\alpha], \mathcal{T}^a[\alpha](s)\} = \Delta^a[\alpha, \beta(s)] [\mathcal{T}[\alpha\sharp\beta] - \mathcal{T}[\alpha\sharp\beta^{-1}]] \quad (2.11)$$

where  $\Delta^a[\alpha, \beta(s)] = \int ds \frac{d\alpha(s)}{ds} \delta^3(\alpha(s), x)$  and  $\alpha\sharp\beta$  refers to the loop that is the union of the two intersected loops  $\alpha$  and  $\beta$ . The inverse  $\beta^{-1}$  refers to inverted direction of the loop  $\beta$  (in performing the parallel transport).

## 2.3 Loop structure

In  $M$ , we consider the graph  $\Gamma$  with  $n$  links  $\gamma_1, \dots, \gamma_n$ . Each links  $\gamma_i$  has a parallel transport  $U_{\gamma_i}$ . Let us consider the functional  $f(U_1(A), \dots, U_n(A))$  on  $SU(2)^n$ . This functional has to be defined with respect to the  $SU(2)^n$  transformations. This symmetry introduces the notion of cylindrical functions, that is  $f(U_1(A), \dots, U_n(A))$  has to be equivalent to a set of cylindrical functions  $\Psi_{\Gamma, f}(A)$ , that is

$$\Psi_{\Gamma, f}(A) = f(U_1(A), \dots, U_n(A)). \quad (2.12)$$

These functions are defined in a Hilbert space and they can be assigned to different graphs by simply guaranty that the new graph  $\hat{\Gamma}$  has no dependence on extra links with respect to  $\Gamma$ . This allows to define the scalar product between any two cylindrical functions  $f$  and  $h$  via

$$\left\langle \Psi_{\Gamma, f}(A), \Psi_{\hat{\Gamma}, h}(A) \right\rangle = \int_{SU(2)^n} dg_1 \dots dg_n \overline{f(g_1 \dots g_n)} h(g_1 \dots g_n) \quad (2.13)$$

such that  $dg$  is defined to be the Haar measure on  $SU(2)$ . These functions are integrable and they belong to a Hilbert space, which we denote as  $\mathcal{H}$ .



## 2.4 Spin Network States

The space  $\mathcal{H}$  is defined to be the largest space with  $n$  copies of  $SU(2)$  subspaces. So it is natural to think about the invariance at the point those subspaces are intersected. This introduces a new subspace in  $\mathcal{H}$  which can be denoted as  $\mathcal{H}_0$  in which we introduce new orthonormal basis called spin network basis. The normalized states in  $\mathcal{H}$  are exactly the traces introduced above, that is

$$\psi_\alpha(A) = \text{Tr}U_\alpha(A). \quad (2.14)$$

Generally (for a multiloop  $\alpha$ ), we write

$$\psi_\alpha(A) = \psi_{\alpha_1}(A) \times \dots \times \psi_{\alpha_n}(A). \quad (2.15)$$

This construction was the first step in the loop gravity program, which was the key to define in more concise and clear form the notion of spin network. For this let us consider the graph  $\Gamma$  with links  $\gamma_i$  such that each link has a color which is, in fact, an associating of an irreducible representation of  $SU(2)$  to that link. The result for this is that we have assigned  $n$   $SU(2)$  irreducible representations to  $n$  links that construct the graph  $\Gamma$ . This is the first assignment. The second assignment comes naturally by the virtue that the coupling of  $n$  irreducible representations of  $SU(2)$  belongs to the subspace  $\mathcal{H}_0$  which introduces the notion of intertwiners, that is at each point of  $n$   $SU(2)$  coupling irreducible representations we assign an intertwiners coloring (intertwiners tensor).

Now, one can see that, for each graph (such as the one displayed in Fig. 2.1), we have a coloring assignment (for the links) and an intertwiners assignment (for the nodes at which the irreducible representations are coupled). This defines the notion of spin network via the triple  $S = \{\Gamma, \vec{s}, \vec{v}\}$  where  $\vec{s}$  refers to the  $n$  coloring assignment, that is  $\{s_i\}$ , and  $\vec{v}$  refers to the intertwiners.

### 2.4.1 Dynamics

The stage now is to solve the Hamiltonian constraints. The well known solution in the literature is the one given by Thiemann [44–46]. The result in that construction (for the Euclidean Hamiltonian  $\hat{H}$ ) is that the action of  $\hat{H}$  on spin network state

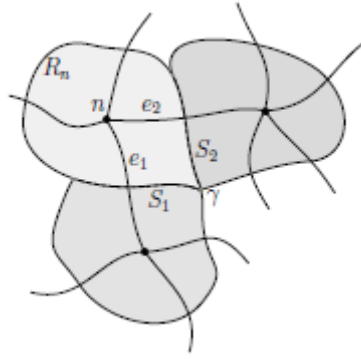


FIGURE 2.1: Spin network graph the corresponding dual picture

$|s\rangle$  takes the form

$$\hat{H} |s\rangle = \sum_i \sum_{(IJ)} \sum_{\epsilon=\pm 1} \sum_{\acute{\epsilon}=\pm 1} A_{\epsilon\acute{\epsilon}}(p_i, \dots, p_n) \hat{D}_{i;(IJ),\epsilon\acute{\epsilon}} |s\rangle \quad (2.16)$$

where  $i$  refers to the nodes of the s-knot  $s$ ,  $(IJ)$  refer to couples of distinct links at  $i$  and  $\hat{D}_{i;(IJ),\epsilon\acute{\epsilon}}$  is an operator acting on  $|s\rangle$  as follows: it creates two additional nodes on the two links  $(IJ)$  and a link of color equals to one relating the two new nodes, also assigns the colors  $p_i + \epsilon$  and  $p_j + \acute{\epsilon}$  to the links between the new nodes and the old node on the which the action of  $\hat{H}$  is considered. The coefficients  $A_{\epsilon\acute{\epsilon}}(p_i, \dots, p_n)$  can be understood in further details reading, for instance, Ref. [1].

It is to be noted that the loop quantum gravity theory aims at studying the quantum nature of spacetime, that is the spacetime itself. So it is expected that the results of the quantization have to be about the discreteness of geometric quantities such as area, volume, angle and length. In fact, in the literature the spectra of those quantities have been found, discussed and investigated:

1. in Ref. [28], the discreteness of the area and volume of space have been discovered. This work was the first result claiming the discreteness of the space measures. In Ref. [11], the authors provided a general formula for the area and volume of space using recoupling theory technology,
2. in [70, 71], the derivation of the area and volume discreteness have been performed using connection formulation of quantum gravity. The results match exactly the previous work by Rovelli and at. el.
3. in Ref. [13], the authors studied the Ashtekar's volume derived in Ref. [71] numerically and analytically.

- 
4. in Ref. [72], the derivation of the volume spectrum has been performed using the discreteness of the length of space. The derivation is a little complicated because of the complexity in computing the length spectrum, but it provides new insights.

# Chapter 3

## Spinfoam

Spinfoam is the modern step achieved in the progress of the loop quantum gravity program. It is investigated and well-studied in both three and four dimensional quantum gravity. This step is the analogous of the Regge discretization of space. However, there is a crucial difference between three and four dimensional theory of gravity since the 3d theory does not have a local degrees of freedom whereas the 4d theory is characterized by this property. In this chapter we study and summarize the current trends of searches in this field by exploring the most attracting and interesting results in the theory.

### 3.1 3 dimensional Euclidean gravity

#### 3.1.1 Kinematical Hilbert space

The theory is defined by groups of elements  $SU(2)$  and the corresponding algebra elements  $su(2)$ . These variables satisfy the relation

$$[U_l, L_l^i] = i(8\pi\hbar G)\delta_{ll'}U_l\tau^i. \quad (3.1)$$

Now, let us consider a graph with  $\Gamma$  with  $L$  links. In this subspace, the truncated Hilbert space can be described via

$$\mathcal{H}_\Gamma = L_2 [SU(2)^L] \quad (3.2)$$

Thus, one can consider an appropriate measure (the Haar measure) and define the following scalar product:

$$\langle \psi | \varphi \rangle = \int_{SU(2)^L} dU_i \overline{\psi(U_i)} \varphi(U_i). \quad (3.3)$$

### 3.1.2 Invariance

Now, let us turn back to the most important point in the theory: the invariance. The above subspace has to be invariant under any symmetry, namely under general gauge transformations elements at the corresponding node Hilbert space. This consideration defines what is known as spin-network states.

Taking into account the invariance amounts to truncate the subspace that represents the invariant part under general gauge transformation which called interwiner. This subspace is symbolized by the notation.

$$\mathcal{K}_L = L_2 [SU(2)^L / SU(2)^N]_L \quad (3.4)$$

Such that  $N$  is the number of nodes,  $L$  number of links and  $\Gamma$  is the graph under study.

### 3.1.3 Basis

There is an important fact characterizing the above structure which is the fact that the links of the graph are  $SU(2)$  rotation generators. This fact reminds us with the theorem by Peter-Weyl, which states with the following orthogonality:

$$\int dU \overline{D_{\hat{m}\hat{n}}^j(U)} D_{mn}^j(U) = \frac{1}{d_j} \delta^{\hat{j}j} \delta_{\hat{m}m} \delta_{\hat{n}n}. \quad (3.5)$$

This relation is the direct consequences of the orthogonality pointed out above and it plays a crucial role in what follows.

For trivalent node Hilbert space, one can see that the invariant part of the space takes the form

$$L_2 [SU(2)^L] = \oplus_{j_i} \otimes_n \text{Inv}_{SU(2)} (\mathcal{H}_{j_1} \otimes \mathcal{H}_{j_2} \otimes \mathcal{H}_{j_3}) \quad (3.6)$$

Such that

$$|j_2 - j_1| \leq j_3 \leq |j_2 + j_1|. \quad (3.7)$$

Using Wigner matrices, the states can be written via

$$\psi(U_l) = \sum_{\substack{j_1 \dots j_L \\ m_1 \dots m_L \\ n_1 \dots n_L}} C_{j_1 \dots j_L m_1 \dots m_L n_1 \dots n_L} D_{m_l n_l}^{j_l}(U_l) \dots D_{m_L n_L}^{j_L}(U_L). \quad (3.8)$$

For the case of three valent node Hilbert space, the function  $C = i^{m_1 m_2 m_3}$  (3jm symbol). Generally, spin network states can be defined via the following relation:

$$\psi(U_l) = \otimes_n i_n \cdot \otimes_l D_{U_l}^{j_l}. \quad (3.9)$$

### 3.1.4 Dynamics

In talking about dynamics we often mean transition amplitude which can be defined after determining the boundaries. Let us consider the two complex deltas. The notion of amplitude is taken from the notion of path integral introduced by Feynman which gives the following formula

$$W_\Delta(U_l) = \mathcal{N} \int dU_e \int dL_f \exp^{\frac{i}{8\hbar\pi G} \sum_f \text{Tr}[U_f L_f]} \quad (3.10)$$

Where  $\mathcal{N}$  stands for normalization. This formula can be simplified as

$$W_\Delta(U_l) = \mathcal{N} \int dU_e \prod_f \delta(U_f). \quad (3.11)$$

Using the identity

$$\delta(U_f) = \sum_j d_j D^{(j)}(U), \quad (3.12)$$

one can show

$$W_\Delta(U_l) = \mathcal{N} \int dU_e \prod_f \left( \sum_j d_j D^{(j)}(U) \right). \quad (3.13)$$

For the case of tetrahedron, this formula reduces to

$$W_\Delta(U_l) = \mathcal{N}_\Delta \sum_{j_f} \prod_f (-1)^{j_f} d_{j_f} \prod_V (-1)^{j_V} \{6j\}. \quad (3.14)$$

This formula completes the covariant derivation.

## 3.2 4 dimensional Lorentzian gravity

Four dimensional Lorentzian gravity is the natural description of quantum gravity since it represents the real world. The starting point is the Holst action which takes the form

$$S[e, w] = \int e \wedge e \wedge \left( * + \frac{1}{\gamma} \right) F \quad (3.15)$$

such that the corresponding (to  $w$ )  $sl(2, C)$ -algebra valued two-form is given by

$$\Pi = \frac{1}{8\pi G} \left( (e \wedge e) * + \frac{1}{\gamma} (e \wedge e) \right), \quad (3.16)$$

and  $e$  is the triads field.

### 3.2.1 Discretization

Let us consider a given triangulation delta of a region of space time (supposed compact). As the case of three dimensional quantum gravity, 4-simplex is the convex hull on four points in four dimensional Euclidean spaces. In the 3d case, the boundaries are 2d areas (triangles). Here the boundaries (which bound the 4-simplex, that is the pentahedron) are tetrahedra. The corresponding two-complex  $\Delta^*$  is defined as follows: at each vertex we consider a 4-simplex (pentahedron), at each edge we consider a tetrahedron and at each face we consider a triangle.

### 3.2.2 Variables

We discretize the variables following the same procedure followed in the case of three dimensional gravity. For this reason we associate  $SL(2, C)$  group element  $U_e$  to each edge  $e$  of the two-complex and  $SL(2, C)$  group element  $U_e$  to each edge  $e$  of the two-complex. The discrete version of this setting is defined via the following

relations:

$$U_e = P \exp \int_e w \in SL(2, C), \quad (3.17)$$

$$B_f = \int_{t_f} B \in sl(2, C). \quad (3.18)$$

### 3.2.3 States

- In defining the states, it will be of worth to give the simplicity constraints which takes the crucial role in quantum theory of gravity in four dimensional space. These constraints take the following formal form:

$$\vec{K} = \gamma \vec{L}, \quad (3.19)$$

where  $\vec{K}$  is defined to be the time component of the four dimensional electric fields,  $\vec{L}$  is the  $so(3)$  rotation generators and  $\gamma$  is the Immirzi parameter.

- An important point to consider in this approach is what is known as the  $Y_\gamma$  map, which takes the following definition: the groups associated with  $SL(2, C)$  belong to the Hilbert space  $V(p, k)$  of the  $(p, k)$  representation which decomposes into the irreducible of the subgroup  $SU(2) \in SL(2, C)$  as follows:

$$V^{p,k} = \bigoplus_{j=k}^{\infty} \mathcal{H}_j \quad (3.20)$$

Such that we have

$$K^2 - L^2 = p^2 - k^2 + 1, \vec{K} \cdot \vec{L} = pk. \quad (3.21)$$

Using the simplicity constraint with the last equations one can get

$$p = \gamma k \quad (3.22)$$

$$k = j \quad (3.23)$$

- So the states of the theory are those of the form

$$|p, k, j, m\rangle = |\gamma j, j, j, m\rangle. \quad (3.24)$$



Therefore, The above map can be written via

$$Y_\gamma : L_2 [SU(2)] \mapsto F [SL(2, \mathcal{C})] \quad (3.25)$$

$$\sum_{jmn} C_{jmn} D_{mn}^j(h) \mapsto \sum_{jmn} C_{jmn} D_{jmjn}^{\gamma j, j}(g) \quad (3.26)$$

### 3.2.4 Transition amplitudes

We follow the same procedure as in the case of 3d gravity. In doing so one can get the following formal form for the amplitude

$$W(h_l) = \int_{SU(2)} dh_{Vf} \prod_f \delta(h_f) \prod_V A_V(h_{Vf}), \quad (3.27)$$

which gives

$$A_V(h_{Vf}) = \sum_{j_f} \int_{SL(2, \mathcal{C})} dg_{Ve} \prod_f (2j_f + 1) \text{Tr}_{j_f} [Y_\gamma^+ g_{eV} g_{Ve} Y_\gamma h_{Vf}]. \quad (3.28)$$

such that

$$\text{Tr}_{j_f} [Y_\gamma^+ g_{eV} g_{Ve} Y_\gamma h_{Vf}] = \sum_{mn} D_{jm, jn}^{\gamma j, j}(g) D_{mn}^j(h). \quad (3.29)$$

This derivation completes the covariant formulation.

# Chapter 4

## Length of Space Quantization

The length of space quantization has been studied canonically through three papers: (a) the Thiemann's length [55], (b) Bianchi's length [56] and (c) Ma's length [57]. The method of the derivation through the three papers is not the same due to the different adopted regularization. Thiemann's derivation characterized by its simplicity and its direct spectrum computation. Bianchi spectrum is a little complicated but has a very clear physical interpretation especially its compatibility with the dual picture of geometry. Ma (and et. al.) derivation present a formula in which new geometric quantities get arisen (the area of space quantization). In addition, it provides two regularizations to end up with the same formula for the length spectrum. Independently, A semiclassical computation of the length of space is performed in Ref. [61]. The results have been compared with those found canonically in Ref. [57]. In this chapter, we investigate the three derivations. We finish the chapter by investigating our strategy in the semiclassical quantization of the length of space.

### 4.1 Bianchi's quantization of the length of space

The starting point in the Bianchi construction is the dual picture of quantum geometry. This picture is available due to the fact that both the area and volume of space are of well known spectra. The point of interest noticed by Bianchi was the fact that: *a node connected to two other nodes identifies two surfaces which intersect at a curve*. The quantization of this curve was the task done by Bianchi.

### 4.1.1 Construction of the length operator

Let consider a three initial data hypersurface  $\Gamma$  (fixed with respect to time) in which we consider the embedded curve  $\gamma$  that is defined as

$$\gamma : [0, 1] \rightarrow \Sigma s \mapsto \gamma^a(s). \quad (4.1)$$

A direct formula to compute the length of such curve can be given as

$$\begin{aligned} L(\gamma) &= \int_0^1 ds \sqrt{\delta_{il} G^i(s) G^l(s)} \\ &= \sqrt{\frac{3}{2}} \int_0^1 ds \sqrt{\delta_{il} \frac{\epsilon^{ijk} \epsilon_{abc} E_j^b E_k^c \dot{\gamma}^a(s) \epsilon^{lmn} \epsilon_{def} E_m^e E_n^f \dot{\gamma}^d(s)}{|\epsilon^{ijk} \epsilon_{abc} E_i^a E_j^b E_k^c|}} \end{aligned} \quad (4.2)$$

where  $\dot{\gamma}^d(s) = \frac{d}{ds} \gamma^d(s)$  and  $G^i = e_a^i(\gamma^a(s)) \dot{\gamma}^a$  corresponds to the pullback of the triad on the curve. Dealing with this expression, one has to overcome two difficulties: the huge kernel in the denominator and the non-polynomial function of the electric field in the numerator. The Overcoming of these difficulties can be achieved using the Tikhonov regularization [73] for the first difficulty and the two-hand operator for the second.

### 4.1.2 Tikhonov Regularization

The problem that facing the construction in Eq. 4.2 is that the volume of space has a huge kernel which makes ill-defined its inversion. So the task is to find via an appropriate regularization the function  $\frac{1}{V} = V^{-1}$  where  $V$  is the volume of  $\Sigma$ . The candidate formula for this expression has to satisfy two conditions: (a)  $V^{-1}$  has to act at nodes and (b) shares the same eigenstates of  $V$ . Thanks to Tikhonov regularization, the following formula for  $V^{-1}$  can be considered as solution:

$$\hat{V}^{-1} = \lim_{\epsilon \rightarrow 0} \left( \hat{V}^2 + \epsilon^2 L_p^6 \right)^{-1} \hat{V}. \quad (4.3)$$

This operator satisfy the above two requirements and make the volume of space inversion well-defined. A remarkable result from this regularization is that once the volume  $V$  is zero its inverse is immediately zero. This result is the most interest part of this regularization since it resolve the problem of inverting non-invertible functions of huge kernel.

### 4.1.3 External Regularization: the Two-Hand Operator

we mean by regularization the way the refinement is performed. The length of space is defined via an integration along the curve. The regularization on this integration will be performed through three steps: (a) replacing the continuous integration in Eq. 4.2 by a Riemann sum,

$$L(\gamma) = \sum_I \Delta s \sqrt{\delta_{il} G_{\Delta s}^i(s_I) G_{\Delta s}^l(s_I)}; \quad (4.4)$$

(b) smearing the area in the numerator over a domain of integration

$$G_{\Delta s}^i(s_I) = \frac{\frac{1}{2} \frac{1}{(\Delta s)^4} \int_{S_I^1} d^2\sigma \int_{S_I^2} d^2\acute{\sigma} V_{x_I}^{ijk}(\sigma, \acute{\sigma}) E_j^a(\sigma) n_a(\sigma) E_k^b(\acute{\sigma}) n_b(\acute{\sigma})}{\sqrt{\frac{1}{48} \frac{1}{(\Delta s)^6} \int_{\partial R_I} d^2\sigma \int_{\partial R_I} d^2\acute{\sigma} \int_{\partial R_I} d^2\acute{\acute{\sigma}} Q}} \quad (4.5)$$

where

$$Q = \left| V_{x_I}^{ijk}(\sigma, \acute{\sigma}, \acute{\acute{\sigma}}) E_i^a(\sigma) n_a(\sigma) E_j^b(\acute{\sigma}) n_b(\acute{\sigma}) E_c^c(\acute{\acute{\sigma}}) n_c(\acute{\acute{\sigma}}) \right|; \quad (4.6)$$

and

$$V_{x_I}^{ijk} = \epsilon^{imn} \mathcal{D}^{(1)}(h_{x_I})_m^j \mathcal{D}^{(1)}(h_{x_I})_n^k \quad (4.7)$$

and finally (c) replacing those integrations (for the areas) by Riemannian sums. In the above analysis, the curve  $\gamma$  has been considered as split into  $n$  sub-intervals via  $\gamma = \cup_I \gamma_I$ .

The result for the length regularization is that this length can be written as sum of finite elementary lengths via the equation

$$L(\gamma) = \lim_{\Delta s \rightarrow 0} \sum_I L_I. \quad (4.8)$$

Combining the above results, one can get the following action for the length of space operator

$$\langle \Psi_{\Gamma, j, i_h} | (\hat{L}^2(\gamma))^2 | \Psi_{\Gamma, j, i_k} \rangle = c \langle h_{12} | \hat{\Lambda}_n \hat{H}_{12} \hat{\Lambda}_n | k_{12} \rangle \quad (4.9)$$

where  $c$  is a constant and  $\hat{\Lambda}_n$  has the following actions

$$\hat{\Lambda}_n | k_{12} \rangle \langle k_{12} | = \frac{\sqrt{12}}{V} | k_{12} \rangle \langle k_{12} | \quad (4.10)$$

and for  $\hat{H}_{12}$  we have

$$\hat{H}_{12} |k_{12}\rangle \langle k_{12}| = (j_1(j_1 + 1)j_2(j_2 + 1) - \rho^2 - \rho) |k_{12}\rangle \langle k_{12}| \quad (4.11)$$

such that  $\rho = \frac{j(j+1) - j_1(j_1+1) - j_2(j_2+1)}{2}$  and  $j(j+1)$  is the casimir of  $k_{12} = j_1 + j_2$ . This formula completes the Bianchi construction of the length of space quantization.

A remarkable feature in the Bianchi construction is that it fits very well in the dual picture of quantum geometry provided by spin network. In the next subsection we will explore the Thiemann's construction of the length of space quantization

## 4.2 Thiemann's quantization of the length of space

Thiemann derived a formula for the length operator of space and its spectrum and eigenfunctions using the key equalities

$$\frac{\delta V}{\delta E_i^a} = e \frac{e_a^i}{2} = \frac{1}{k} \{A_a^i, V\} \quad (4.12)$$

where  $V$  is the total volume of an initial data hypersurface  $\Sigma$ ,  $e_a^i$  is a triad field with inverse  $e_i^a$ ,  $e = \text{sgn}(\det(e_a^i))$ ,  $E_i^a = \det(e_b^j) e_i^a$ ,  $k$  is Newton's constant and  $E_a^i$  is a  $SU(2)$  connection. Together with the fact that the total volume  $V$  of  $\Sigma$  can be quantized in a mathematically rigorous way, the Thiemann's length spectrum becomes well-defined.

### 4.2.1 Regularization

Setting a base in  $su(2)$  by  $\tau_i = -i\sigma_i/2$  ( $\sigma_i$  are Pauli matrices) such that  $e_a = e_a^i \tau_i$  and  $A_a = A_a^i \tau_i$ , using the expansion (for small  $A_a$ )  $h_e(A_a) = 1 + A_a + 0(A_a^2)$  and the key equality

$$q_{ab} = -2\text{Tr}(e_a e_b) = -\frac{8}{k^2} \text{Tr}(\{A_a, V\} \{A_b, V\}) \quad (4.13)$$

the regularization becomes an easy task: we replace the integration in the following expression

$$L(\gamma) := \int_{[0,1]} ds \sqrt{\dot{\gamma}^a(s) \dot{\gamma}^b(s) q_{ab}(\gamma(s))} \quad (4.14)$$

by a Riemann sum and substituting in it the expression of  $q_{ab}(\gamma(s))$ . This amounts to subdivide the interval  $s \in [0, 1]$  into  $n$  subdivisions and taking the sum, that is

$$L_n(\gamma) := \frac{1}{k} \sum_{i=1}^n ds \sqrt{\text{Tr}(\{h_i, V\} \{h_i^{-1}, V\})}. \quad (4.15)$$

This formula gives the lengths spectrum when it is considered in the limit  $n \rightarrow \infty$ , that is

$$L(\gamma) := \lim_{n \rightarrow \infty} L_n(\gamma) \quad (4.16)$$

Computing length of space spectrum using this formula amounting to compute the actions of the commutators inside the square root on cylindrical functions.

A remarkable feature in the Thiemann's construction is that it does not suffer from non-invertible functions of huge kernel.

## 4.2.2 The Spectrum

The last equation defines completely the length of space spectrum in the sense that the volume of space is of a well known action on cylindrical functions. Using eq.(88) we get

$$\frac{1}{8} \hat{L}^2(\gamma) = \left[ \text{Tr}(h^{-1} \hat{V} h) \hat{V} + \hat{V} \text{Tr}(h^{-1} \hat{V} h) \right] + 2\hat{V}^2 + \text{Tr}(h^{-1} \hat{V}^2 h) \quad (4.17)$$

For the case of trivalent spin network, the three first terms vanish identically, the computation restricted to the last term. In Thiemann's paper of the length quantization this spectrum is given explicitly by the following formula

$$L(\gamma) = \frac{l_p \sqrt{(j_3 + 1)\lambda}}{2\sqrt{j_3 + \frac{1}{2} + j_3 \eta}} \quad (4.18)$$

here  $\lambda = \sqrt{(j_1 + j_2 + j_3 + 2)(j_1 + j_2 - j_3)(-j_1 + j_2 + j_3 + 1)(j_1 - j_2 + j_3 + 1)}$  and  $\eta = \sqrt{(j_1 + j_2 + j_3 + 1)(j_1 + j_2 - j_3 + 1)(-j_1 + j_2 + j_3)(j_1 - j_2 + j_3)}$ . In this formula and for a bi-valent vertex such that  $j_1 = j_2 = j_0$  we get  $L(\gamma) = l_p \sqrt[4]{j_0(j_0 + 1)}$  which gives for the minimal case, that is  $j_0 = 1/2$ , the minimal length value  $\frac{1}{\sqrt{2}} \sqrt[4]{3} l_p$ .

the result by Thiemann can be stated as follows: *The length of space can change only in packets of  $\delta L = \pm \frac{1}{2} \frac{1}{\sqrt{j_0}} l_p$  which (for large spin) looks like a continuous operator.*

### 4.3 Ma's quantization of the length of space

Ma derived the length spectrum in a slightly analogous way to the one shown in Ref.[56] but in terms of an additional geometric quantity, the angle spectrum that was derived in Ref.[74]. The derivation was shown using two regularizations, that was introduced in Ref.[75] and that in Ref.[76], to end up with the same spectrum formula.

The derivation has been shown for the case of four valent spin network. To fully explore the the explicit formula, we have to have a prior knowledge of:

1. the direction of space spectrum which can be written as

$$\sin \phi_v^{12} = \sqrt{1 - \left( \cos \left( \frac{j_{12}(j_{12} + 1) - j_1(j_1 + 1) - j_2(j_2 + 1)}{2\sqrt{j_1(j_1 + 1)j_2(j_2 + 1)}} \right) \right)^2} \quad (4.19)$$

where  $\phi_v^{12}$  is the spectrum that represents the angles between the vectors corresponding to  $j_1$  and  $j_2$  such that  $j_2 - j_1 \leq j_{12} \leq j_1 + j_2$ , the index  $v$  refers to the fact that the three corresponding operators to  $j_1, j_2$  and  $j_{12}$  are coupled at the vertex  $v$ .

the volume of space  $V$  spectrum, which has a well known action on cylindrical functions.

With this, the spectrum of the length of space shown in Ref.[57]. can be simplified much by the following expression

$$L(\gamma) = \frac{\sqrt{j_1(j_1 + 1)}\sqrt{j_2(j_2 + 1)}\sqrt{1 - \left( \cos \left( \frac{j_{12}(j_{12} + 1) - j_1(j_1 + 1) - j_2(j_2 + 1)}{2\sqrt{j_1(j_1 + 1)j_2(j_2 + 1)}} \right) \right)^2}}{V}. \quad (4.20)$$

This formula completes the (Ma and et. al.)'s construction. The authors found this result via two regularization, which makes its argument more strength. The spectrum found via this last equation will be compared with our result of the semiclassical quantization of the length of space derived in the next subsection (by us).

## 4.4 Semiclassical Quantization of the Length of Space

All of the three derivations demonstrated above three subsections lies in the notion of the regularization of space and the action of the geometric quantities operators on cylindrical functions.

In this quantization, however, we will not talk about the regularization of space and cylindrical functions because this is naturally included in the relation between the quantum polyhedra and loop gravity. In fact, the point of interest the present work lies in is a simple relation relating the length of the tetrahedral edges with the volume and areas, which is obtained by restricting the bulkback of triads on curves to the case of the quantum tetrahedra. Together with the fact that the volume of space has a well-known semiclassical spectrum, one can quantize semiclassically the length from Bohr Sommerfeld quantization.

### 4.4.1 Tetrahedra Space of Shapes

tetrahedron space of shapes can be fully explored, suing the results obtained from Refs. [77, 78], via the pair  $(p, \varphi)$  which defines the phase space of tetrahedron. Performing BSQ on it results the quantum tetrahedron. For the present work, however, BSQ quantization will not be performed directly, it will be tacitly taken in the calculations (for the volume spectrum) since the point of interest here is the quantization of the length of space in which the integration of a symplectic area (as it will be clear later) does not appear.



### 4.4.2 The Length of Space Quantization

As our quantization is rather semiclassical, the length of space meant here is the length of a tetrahedral edge  $L$ . To proceed, let us consider the euclidean 3d space  $\xi(\alpha, \beta, \lambda)$  where  $\alpha$ ,  $\beta$  and  $\lambda$  are its dimensions and  $\partial\xi(\alpha(\lambda), \beta(\lambda))$  its slices, in which we localize the  $\xi$ 's three coordinates associated with a tetrahedron  $\tau$  by bounding them in intervals such that  $0 \leq \alpha \leq \alpha_0, 0 \leq \beta \leq \beta_0$  and  $0 \leq \lambda \leq \sigma$ . the  $\tau$ 's areas  $A_1, A_2, A_3$  and  $A_4$  can be defined by choosing a basis at a corner  $c$  in  $\tau$  of three unit vectors  $u_\alpha, u_\beta$  and  $u_\lambda$  such that  $\vec{A}_1 = \frac{1}{2}\alpha_0\beta_0(u_\alpha \times u_\beta)$ ,  $\vec{A}_2 = \frac{1}{2}\alpha_0\sigma(u_\alpha \times u_\lambda)$ ,  $\vec{A}_3 = \frac{1}{2}\beta_0\sigma(u_\lambda \times u_\beta)$  and  $\vec{A}_4 = -(\vec{A}_1 + \vec{A}_2 + \vec{A}_3)$ .

Let us now proceed into the quantization. By combining the following two key observations:

1. The volume of space has a well-defined semiclassical spectrum via the framework in Ref.[28];
2. the length  $L(\gamma) = \int_0^1 ds \sqrt{\delta_{il} G^i(s) G^l(s)}$  for the quantum tetrahedra can be defined via

$$L = \frac{2}{3} \frac{|\vec{A}_1 \times \vec{A}_2|}{\sqrt{Q}} \quad (4.21)$$

where  $Q$  is the squared volume of  $\tau$ , the computation of length spectrum is an easy task. This amounts to promoting the volume, area and angle in the last equation into operators, that is

$$\hat{L} = \frac{2}{3} \frac{\hat{A}_1 \hat{A}_2 \sin \hat{\theta}}{\sqrt{\hat{Q}}}. \quad (4.22)$$

where  $\theta$  is the angle between  $\vec{A}_1$  and  $\vec{A}_2$  and the hat  $\hat{\phantom{x}}$  refers to the operator. The fully semiclassically computation of  $\hat{L}$  via the last equation requires a prior knowledge of the spectra of both  $\hat{Q}$  and  $\hat{\theta}$ . Those were studied very well in the literature and they are summarized in of the following subsections

#### 4.4.2.1 The volume of space quantization

In Ref.[28], the discreteness of the volume of space from Bohr-Sommerfeld quantization was performed. The basic idea in this framework is that the volume of space has been considered as playing the role of Hamiltonian generating classical orbits

together with the fact that Bohr-Sommerfeld orbits encircle symplectic areas that is  $2\pi \left(n + \frac{1}{2}\right)$  times the Planck constant. The resulted spectrum for the volume of space matches well the one found canonically in loop gravity. This framework has been investigated in further details in Ref.[29], in which some data of the volume spectrum found semiclassically and canonically are presented and compared. The relevance of this framework to the present work is that the resulted spectrum of the volume will be used directly here in the computation of the length spectrum by using Eq. (4.22).

#### 4.4.2.2 The angle of space quantization

In Ref. [74], the author introduced an operator for the angle of space and its spectrum via an appropriate regularization. The derivation is based solely on canonical arguments and the spectrum has a simple and nice formula which can be written as

$$\phi_v^{12} = \arccos \left( \frac{j_{12}(j_{12} + 1) - j_1(j_1 + 1) - j_2(j_2 + 1)}{2\sqrt{j_1(j_1 + 1)j_2(j_2 + 1)}} \right). \quad (4.23)$$

where  $\phi_v^{12}$  is the spectrum that represents the angles between the vectors corresponding to  $j_1$  and  $j_2$  such that  $j_2 - j_1 \leq j_{12} \leq j_1 + j_2$ , the index  $v$  refers to the fact that the three corresponding operators to  $j_1, j_2$  and  $j_{12}$  are coupled at the vertex  $v$ .

This spectrum is used properly when the study is based solely on canonical arguments, but as our quantization to the length of space is rather semiclassical, one has to derive that spectrum semiclassically. This task can be done using Heron's formula and the equidistant spacing spectra for the areas. For the triple  $\vec{A}_1, \vec{A}_2$  and  $\vec{A} = \vec{A}_1 + \vec{A}_2$ , we have

$$\varphi = \arcsin \left( \frac{\sqrt{(A_1 + A_2 + A)(A_1 + A_2 - A)(A_1 - A_2 + A)(-A_1 + A_2 + A)}}{2A_1A_2} \right). \quad (4.24)$$

where  $\varphi$  is the angle between  $\vec{A}_1$  and  $\vec{A}_2$ ,  $A_1 = j_1 + \frac{1}{2}$  and  $A_2 = j_2 + \frac{1}{2}$ .

TABLE 4.1: Comparison of the Bohr-Sommerfeld and loop gravity length spectrum. The tetrahedral areas are assumed quantized equidistantly via  $A_i = j_i + \frac{1}{2}, i = \overline{1,4}$ . The tetrahedral volume used in computing the length spectrum was computed separately for both the semiclassical and canonical derivation.

$j_1$	$j_2$	$j_3$	$j_4$	Bohr-Sommerfeld length spectrum	Loop gravity length spectrum	Accuracy
0.5	0.5	0.5	0.5	3.436	2.279	33 %
				0.0	0.0	exact
0.5	0.5	0.5	1.5	0.0	0.0	exact
0.5	0.5	1.0	1.0	2.517	1.783	29 %
				0.0	0.0	exact
0.5	0.5	1.0	2.0	0.0	0.0	exact
0.5	0.5	1.5	1.5	2.133	1.524	28 %
				0.0	0.0	exact
0.5	0.5	1.5	2.5	0.0	0.0	exact
0.5	1.0	1.0	2.5	0.0	0.0	exact
0.5	0.5	2.0	2.0	1.890	1.355	28 %
				0.0	0.0	exact
1.0	1.0	1.0	2.0	3.745	2.791	25 %
				2.368	2.791	15 %
1.0	1.0	1.0	3.0	0.0	0.0	exact
0.5	0.5	2.5	2.5	1.718	1.233	28 %
				0.0	0.0	exact

#### 4.4.2.3 The length of space quantization

: The length of space quantization means the statement that the  $\tau$ 's edges lengths have to be varied in discrete steps and consistently with the discrete variation of the areas, volume and angles since the edges lengths depend only on these. By combining the above results, the length spectrum takes the formula

$$L = \frac{\sqrt{(A_1 + A_2 + A)(A_1 + A_2 - A)(A_1 - A_2 + A)(-A_1 + A_2 + A)}}{3\sqrt{Q}}. \quad (4.25)$$

The numerator presents no problem since its spectra are well-defined. The denominator presents a serious problem: in fact, the volume of space has a huge kernel which makes the length spectrum ill-defined. However, one can adopt the regularization of Tikhonov discussed in Ref.[73] (as it was done in ref.[55]) canonically and the action of this regularization on polyhedra is naturally included in the relation between the quantum polyhedra and loop gravity. The result of this regularization is that when the volume of space equals to zero then the length of space is immediately zero. This overcomes the problem of kernel and makes the length spectrum well-defined.

In summary, this chapter shows the discreteness of the length of space from Bohr-Sommerfeld quantization. The resulted spectrum has a nice and simple formula summarized in eq. (5.35). The fully computation of this spectrum requires a prior determination of the spectrum of the volume  $\sqrt{Q}$ , which is the task done in ref.[28]. Some values of the spectrum found via the method of the present work compared with those found canonically in Ref.[57] are shown in Table 4.1, above.

The accuracy values shown in this table present some deviation between the two spectra. In fact, this deviation can be traced back to the fact that the equidistant spacing spectrum of the tetrahedral areas used in the semiclassical derivation does not match well (for small values of the area) the standard spectrum derived canonically in loop gravity.

# Chapter 5

## The quantum polyhedra

Loop quantum gravity (LQG) has taken its attraction extensively during the last years. This fact is not of a surprising matter and it is expected due to the fact it comes via three different roads to end up with the same results such as the discreteness of the space measurements like volume, area, angle and length. In this chapter we describe the geometric approach which has got clear after the the paper entitled *Polyhedra in loop quantum gravity* has been published. Here we summarize the main results and present our contribution in the quantum polyhedron, by studying a new quantum geometric object called the quantum trihedron.

Starting from two key results:

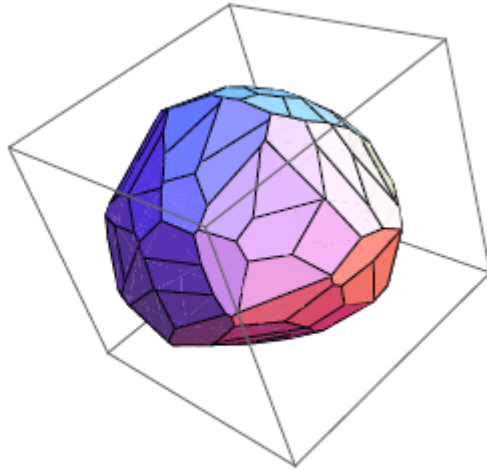
1. the physical space  $\mathcal{H}_F$  of spin network at a node  $n$  with  $N$  valence is equivalent to the quantization of a classical phase space  $S_N$  called Kapovich-Millson phase space (KMPS);
2. there is unique polyhedron at each point in  $S_N$  with given areas,

one can explore the following results

$$\text{polyhedra with } F \text{ faces} \leftrightarrow \text{classical phase space } S_F \leftrightarrow \text{intertwiner space } \mathcal{H}_F \quad (5.1)$$

### 5.1 The phase space of polyhedra

Let us consider a set of  $N$  non-co-planar vectors (see Fig 5.1)  $\{F_i = A_i n_i\}$  such that the condition  $\sum_{i=1}^N F_i = 0$  holds, then the Minkowski theorem states that:

FIGURE 5.1: Polyhedron with  $N$  faces

there is a unique bounded convex polyhedron (up to translations and rotations  $SO(3)$ )  $p$  having those areas as faces.

According to Kapovich and Milson, the set  $\{F_i = A_i n_i\}$  has the structure of a symplectic manifold. In this space, we have a set of  $(N - 3)$  pairs  $(\theta_i, \mu_i)$  of action-angle variables with canonical Poisson brackets.

In the field of polyhedra shapes, there are several possible ways to visualize the possible figure that can be constructed via  $N$  areas vectors. This introduces the notion of classes. The case of tetrahedron is trivial since there is only one possible shape can be constructed via four areas vectors. The first non-trivial case is the one corresponding to the possible shapes that can be constructed via five areas vectors, that is  $N = 5$ . For this case, there are two shapes: triangular prism and pyramid. In this case also, there is a notion of *dominant class* which is here corresponds to the triangular prism. The dominant class is that which has the maximum number of vertices. For the case of  $N = 6$ , there are seven different classes and the dominant is the one named as *cuboid*.

## 5.2 Polyhedra from areas and normals

By the title of this subsection we mean the way to measure the lengths of polyhedra edges and their volume. This task is done via an algorithm called Lasserre's procedure Ref.[79]. In Ref.[27], this algorithm is investigated in further details. It gives the lengths of polyhedra edges and their volume. This construction can be used in numerical study as well as analytical study.

## 5.3 Relation to loop quantum gravity

The relation between the quantum polyhedron and loop gravity has a crucial role in adopting the geometric approach in LQG. In fact, this adoption simplifies very much our understanding of LQG especially its applications and the practical dealing with it.

The authors in Ref.[27] studied this relation via two key observations:

- *Intertwiners are the building blocks of spin-network states*
- *Intertwiners are the quantization of the phase space of Kapovich and Millson.*

Therefore, spin network can be understood as a collection of quantum polyhedra at each vertex.

## 5.4 The quantum tetrahedron

In Ref.[28], the authors studied the quantization of the volume of space (tetrahedron volume) using Bohr Sommerfeld quantization. This study can be considered as a special case in talking about the quantum polyhedra, but it was of great interest since it sounds like a good example to understand better the quantum polyhedra (via the generalization). The central result by the authors is the good matching of the volume spectrum of space with the canonical derivation. The agreement is extremely well for large values of tetrahedron's areas values. In small values of the areas, some deviation is remarked. However this can be traced back to the fact that the equidistant area spectrum of the areas of tetrahedron does

not match well (for small values) the standard one derived canonically. In this quantization, two key observations are considered:

- the volume of space it taken as playing the role of Hamiltonian generating classical orbits;
- the Planck hypothesis: symplectic areas vary in discrete steps and they are  $2\pi(n + \frac{1}{2})$  times the Plank constant.

## 5.5 Bohr-Sommerfeld quantization

Bohr-Sommerfeld quantization (BSQ) or old quantum theory applied on completely integrable Hamiltonian systems. The energy spectrum of the hydrogen atom obtained by Sommerfeld agrees exactly with the observation. The problem with Bohr–Sommerfeld theory is that it does not provide a way to discuss the probability of transition between states. So the next stage in improving the model was the matrix theory of Heisenberg [80] and the wave theory of Schrodinger [81]. Heisenberg’s approach was further developed by Born and Jordan [82]. Dirac [82] showed that the theories of Heisenberg and Schrodinger are equivalent.

### 5.5.1 Old quantum theory

1. The main tool in the old quantum theory has been Bohr–Sommerfeld quantization: the statement that there are just limit discrete of states of a classical integrable motion as allowed states. The basic principle in this predating theory (to the modern quantum mechanics) is Bohr-Sommerfeld quantization (BSQ) condition:

$$\oint p_i dq_i = n_i h \quad (5.2)$$

where  $(p_i, q_i)$  are pairs of canonically conjugated variables and  $n_i$  is an integer.

2. *De Broglie waves*: in 1924, Broglie suggested that all matter are described by waves obeying the relations.

$$p = \hbar k \quad (5.3)$$



where  $k$  is the wave-number of a wave. Performing BSQ condition with this prediction gives the statement: the matter waves only takes discrete frequencies or discrete energy levels. This was the heuristic starting point into the Schrodinger equations.

Some limitations to note on the old quantum theory are: (a) we can not (using it) calculate intensities of the spectral lines, (b) Zeeman effect is not explainable and (c) does not explore chaotic behaving. Thus, the old quantum theory has been known as semi-classical approximation to the standard quantum mechanics.

## 5.5.2 Heisenberg Representation

In 1925, Werner Heisenberg derived and introduced a new formulation for quantum mechanics. A remarkable feature which characterizes this representation is that the operators incorporate a dependency on time and the states not. It differs from the Schrodinger representation in that it can be achieved via passive and active transformation. In addition, the Heisenberg transformation can be seen as the matrix formulation of the quantum mechanics.

In this representation, the observables have to satisfy the following equation

$$\frac{dA}{dt} = \frac{i}{\hbar} [H, A(t)] + \left( \frac{\partial A}{\partial t} \right)_H \quad (5.4)$$

Such that  $H$  is the Hamiltonian. The equivalence between this representation and that of Schrodinger can be explored via Stone–von Neumann theorem, which proves that those two representations are nothing than two unitarily equivalent representations.

### 5.5.2.1 Mathematical derivation

Let us start by giving the meaning of the expectation value. For an observable  $o$  which is a Hermitian linear operator defined via a state  $\chi$  at a given moment of time  $t$ , the expectation value of  $o$  takes the form

$$\langle A \rangle_t = \langle \psi | A(t) | \psi \rangle \quad (5.5)$$

Now, let us borrow the idea by Schrodinger which declare that the relation between two states defined at two different times  $t_1$  and  $t_2$  is given by the relation

$$|\psi(t) = U(t)|\psi(t = 0)\rangle \quad (5.6)$$

where

$$U(t) = e^{-iHt/\hbar}, \quad (5.7)$$

(H is supposed time-independent). This gives the following

$$A(t) := e^{iHt/\hbar} A(t = 0) e^{-iHt/\hbar} \quad (5.8)$$

Which allows in turn to derive the following

$$\frac{dA}{dt} = \frac{i}{\hbar} [H, A(t)] + e^{iHt/\hbar} A(t = 0) e^{-iHt/\hbar} \left( \frac{\partial A}{\partial t} \right) e^{iHt/\hbar} A(t = 0) e^{-iHt/\hbar} \quad (5.9)$$

Via the relation between Poisson brackets and commutators

$$\frac{i}{\hbar} [H, A(t)] \equiv i\hbar \{H, A(t)\} \quad (5.10)$$

we get (when A is supposed time independent)

$$\{H, A(t)\} = \frac{dA}{dt} \quad (5.11)$$

### 5.5.2.2 Matrix mechanics

In 1925, Werner Heisenberg, Max Born, and Pascual Jordan derived a new formulation for quantum mechanics called now “matrix mechanics”. This was the first successful attempt into a quantum word describing nature and the consistent picture conceptually.

#### The basic idea

In fact, the birth of the quantum mechanics was not with Heisenberg, it was with what is known as the *old quantum theory*. Which states that classical orbits

encircles symplectic areas that are  $2\pi n$  times the Planck constant, that is

$$\int_T^0 P dX = nh \quad (5.12)$$

The problem with this formulation is that it does not include the evolution in time. The first remark was made by Heisenberg is that the position  $X$  is periodic which allow us to use what is known as Fourier analysis, that is the position can be expanded via Fourier series via the relation

$$X(t) = \sum_{-\infty}^{n=0} e^{2\pi i n t/T} X_n \quad (5.13)$$

Any orbit describes an energy level, say  $H_n$ . So if we pick up two levels  $H_n$  and  $H_m$  one can see that there is a difference between them which describes an energy of radiation characterizing the emission or absorption of a photon in the transition between the two levels which has the value  $H_m - H_n$ . Now one can see that the two orbits can be described via two systems of coordinates  $X_m$  and  $X_n$  or simply  $X_{mn}$ . Those coordinates can be, in fact, written using the relation

$$X_{mn}(t) = e^{2\pi i (E_n - E_m)t/h} X_{nm}(0) \quad (5.14)$$

This allows deducing another quantity called momentum matrix  $P_{mn}$  and its product with the position matrix can be defined via the criteria of multiplication in matrix analysis, that is we have

$$(XP)_{mn} = \sum_{k=0}^{\infty} X_{mk} P_{kn} \quad (5.15)$$

Notice that the product is not necessarily commute which is the remarkable property characterizing operators in the quantum theory of modern physics.

On the other hand, one can express the uncertainty principle using the following relation

$$\sum_{k=0}^{\infty} (X_{nk} P_{km} - P_{nk} X_{km}) = \frac{i\hbar}{2\pi} \delta_{mn} \quad (5.16)$$

### 5.5.3 Canonical commutation relations

Let first write the action integral using matrix language. This can be achieved via the relation

$$\int_0^T \sum_k P_{mk} \frac{dX_{kn}}{dt} dt = T_{mn} \quad (5.17)$$

The derivation with respect to  $j$  gives (after a straightforward calculations)

$$\frac{2\pi}{T} \int_0^T dt \left( \frac{dp}{dj} \frac{dX}{d\theta} - \frac{dX}{dj} \frac{dp}{d\theta} \right) \quad (5.18)$$

This is the commutation relation between  $J$  and the evolution parameter (time). It corresponds to the commutation relation between time and energy.

#### 5.5.3.1 Transformation theory

As in the case of the ordinary space of dimensions, in phase space there are transformations which preserves the Poisson structure which called transformation theory. Those transformations can be defined via the following system of equations

$$x \mapsto x + dx = x + \frac{\partial H}{\partial p} dt, \quad (5.19)$$

$$p \mapsto p + dp = p - \frac{\partial H}{\partial x} dt. \quad (5.20)$$

For a general function  $A$  of  $x$  and  $p$ , one can write

$$dA = \frac{\partial A}{\partial x} dx + \frac{\partial A}{\partial p} dp = \{A, G\} ds, \quad (5.21)$$

where  $G$  (Hamiltonian) is known as the infinitesimal generator of the canonical transformation. The integration of the last equation gives

$$\acute{A} = U^+ A U \quad (5.22)$$

where

$$U = e^{iGs} \quad (5.23)$$

### 5.5.4 Symmetry

If we consider  $L$  as generators of symmetry, then one can expect the following

$$\frac{dH}{ds} = i[H, H] = 0 \quad (5.24)$$

$$\frac{dL}{ds} = i[L, H] = 0 \quad (5.25)$$

This means that  $L$  is constant and conserved like the energy.

## 5.6 The Quantum Trihedron

In Ref. [28], the Bohr-Sommerfeld quantization (BSQ) of tetrahedron has been performed using the Kapovich Millson phase space (KMPS). The tetrahedron's areas were assumed quantized equidistantly. The consistency of this assumption with the quantization of space using KMPS has not been fully explored. However, this consistency has to be checked because adapting this assumption without checking the proof can be seen as a limitation.

Therefore, attempting to extend the quantization using KMPS to the case of the area of space will be an important step. The present work provides a clear proof to that assumption by proving that the only spectrum for the tetrahedron's areas (using KMPS) is that of equidistant spacing. The key idea to explore this result is to consider the tetrahedron's areas as boundaries for the volume and the limit to these boundaries has to be taken after the quantization, namely after performing BSQ.

The physical interpretation of the result is simple: the KMPS for the bulk tetrahedron reduces to two points for a given boundary area and the quantization means, in fact, that the length of the line relates the two points varies in discrete steps. The remarkable feature in this analysis (as it will be clear later) is that one can quantize semi-classically both the area and volume of space consistently using only KMPS within BSQ.

### 5.6.1 The Areas and Volume of Tetrahedron as Boundaries and Bulk

In Minkowski theorem, the vectors that represent the areas of a convex polyhedron must satisfy two properties: the non-co-planarity and the closure constraint. For a tetrahedron  $\tau$ , the convex hull on four points can be represented by four areas  $A_1, A_2, A_3$  and  $A_4$ , which can be defined in 3d space  $\xi(\beta, \alpha, \lambda)$ , where  $\beta, \alpha$  and  $\lambda$  are its dimensions and  $\partial\xi(\alpha(\lambda), \beta(\lambda))$  its slices. In the context of this space, we attempt to localize the  $\tau$ 's areas and its volume. One can define the  $\tau$ 's covered region (by the convex hull) by bounding the three associated coordinates  $\beta, \alpha$  and  $\lambda$  in intervals, that is  $0 \leq \alpha \leq \alpha_0, 0 \leq \beta \leq \beta_0$  and  $0 \leq \lambda \leq \sigma$ . We restrict  $\sigma$  to be defined in the neighborhood of  $\lambda = 0$ , then the quantum volume of  $\tau$  will be restricted to its minimal value in spectrum, which corresponds to the largest phase space orbit. In addition, we suppose (for simplicity) that the angle between the two vectors  $\vec{A}_1$  and  $\vec{A}_2$  and that between  $\vec{A}_1$  and  $\vec{A}_3$  is  $\frac{\pi}{2}$  and  $A_2 = A_3$ .

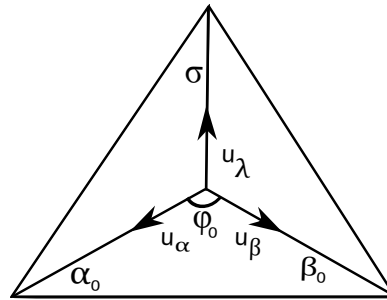


FIGURE 5.2: A parametrized tetrahedron  $\tau(\sigma)$  at the minimum value of its volume (with respect to the variation in  $\sigma$ ) in spectrum, such that  $\sigma$  is defined in the neighborhood of  $\lambda = 0$ .

The quantities  $\alpha_0, \beta_0$  and  $\sigma$  represent (for  $\tau$ ) tetrahedral edges (see Fig. 5.2) and they are defined as functions of the tetrahedron's volume conjugate variable  $\eta$ . In addition,  $\sigma$  is defined as function of  $\lambda$ . The dependence of  $\sigma$  on  $\lambda$  refers to the maximum value of  $\lambda$  and its dependence on  $\eta$  refers to the dynamics (orbital evolutions in the space of shapes  $\mathcal{P}_{\tau(\sigma)}$ ). Therefore, varying  $\sigma$  refers to the jumping from an eigenvalue of the tetrahedron's volume into the next one. For large values of the volume, this jumping will be considered (for the maximum value of the coordinate  $\lambda$ , that is  $\sigma$ ) as differentiation.

The areas of  $\tau$  can be defined by choosing a basis in  $\xi(\beta, \alpha, \lambda)$  of three unit vectors  $u_\alpha, u_\beta$  and  $u_\lambda$  supported by the three edges  $\alpha_0, \beta_0$  and  $\sigma$  at a corner in  $\tau$  such

that  $\vec{A}_1 = \frac{1}{2}\alpha_0\beta_0(u_\alpha \times u_\beta)$ ,  $\vec{A}_2 = \frac{1}{2}\alpha_0\sigma(u_\alpha \times u_\lambda)$  and  $\vec{A}_3 = \frac{1}{2}\beta_0\sigma(u_\beta \times u_\lambda)$ , where  $\alpha_0 = \alpha(\lambda = 0)$  and  $\beta_0 = \beta(\lambda = 0)$ . If we tend  $\sigma$  to zero then  $\vec{A}_2 \cong \vec{0}$ ,  $\vec{A}_3 \cong \vec{0}$  and  $\vec{A}_1 \cong \vec{A}_4$ . These considerations will be the key to study the quantization of the tetrahedron's areas using the KMPS boundary.

### 5.6.2 The Quantization

By the quantization, we mean our looking for the spectra of the tetrahedron's areas, which have only one value (one level for the Hamiltonian) due to the fact that the tetrahedron's areas were fixed first. In doing so, we adapt two distinct strategies, which give surprisingly the same result, equidistant areas spectra. The Planck hypothesis is used formally in the first strategy and modified slightly in the second one:

- In the first strategy, the quantization of the  $\tau$  areas will be obtained as a quantum limit, namely after performing the quantization, to the boundaries of the  $\tau$ 's quantum volume, that is we will take the encircled symplectic area (by Bohr-Sommerfeld orbits) as times of the Planck constant (for the tetrahedral phase space) and then the limit to the boundaries ( $\tau$ 's KMPS boundary) will correspond, as consequence, a symplectic line taken as times the Planck constant.
- In the second strategy, we determine the KMPS boundaries, which are (as we will see later) two points. Then, the Hamiltonian of our system ( $\tau$ 's boundaries) will be considered as the  $\tau$ 's areas. The symplectic area reduces to a line. The Planck hypothesis (BSQ condition) will be reduced as: *the lengths of encircled lines (bounded) by two phase space points in a one dimensional symplectic space vary in discrete steps, that is  $2\pi(n + \frac{1}{2})$  times the Planck constant.*

### 5.6.3 The first strategy

In Ref. [28], the authors handled the discreteness of the volume of space from BSQ using KMPS. In the present work, we deal with the discreteness of the area using the boundary of the tetrahedron's KMPS. To proceed, we first give a brief summary to the key results that allow one to define the phase space variables

of the theory. The first result is a theorem due to Minkowski which states that for  $M$  non-co-planar unit vectors  $\{\vec{n}_M\}$  and  $M$  positive numbers  $\{A_M\}$  such that the closure condition  $\sum_{k=1}^M A_k \vec{n}_k = \vec{0}$  holds, then the areas  $\{\vec{A}_M = A_M \vec{n}_M\}$  fully characterize the shapes of a geometrical object called polyhedron (up to rotations and translations, this polyhedron is unique). This allows to define the space of shapes of polyhedron  $\mathcal{P}_M$  to be

$$\mathcal{P}_M = \left\{ \vec{A}_k, k = 1, \dots, M \mid \sum_{k=1}^M A_k \vec{n}_k = \vec{0}, |\vec{A}_k| = A_k \right\} / SO(3). \quad (5.26)$$

; (b) the so-called Kapovich-Millson phase space: As it is shown in the quantum polyhedron paper, the set  $\mathcal{P}_m$  has a symplectic structure. The Poisson brackets between two arbitrary functions  $F(\vec{A}_l)$  and  $G(\vec{A}_l)$  can be defined via

$$\{F, G\} = \sum_{l=1}^h \vec{A}_l \cdot \left( \frac{\partial F}{\partial \vec{A}_l} \times \frac{\partial G}{\partial \vec{A}_l} \right). \quad (5.27)$$

The second result is the so-called Kapovich-Millson phase space: As it is shown in Refs. [27, 28], the set  $\mathcal{P}_M$  has a symplectic structure. The Poisson brackets between two arbitrary functions  $F(\vec{A}_l)$  and  $G(\vec{A}_l)$  can be defined via

$$\{F, G\} = \sum_{l=1}^M \vec{A}_l \cdot \left( \frac{\partial F}{\partial \vec{A}_l} \times \frac{\partial G}{\partial \vec{A}_l} \right). \quad (5.28)$$

The variables that satisfy the equations  $\{p_m, q_n\} = \delta_{mn}$  are defined as follows: the momenta variables are the norms  $|\vec{p}_m| = \left| \sum_{l=1}^{m+1} \vec{A}_l \right|$  where  $m = 1, \dots, M$ , the coordinates variables is the angles between the vectors  $\vec{p}_m \times \vec{A}_{m+1}$  and  $\vec{p}_m \times \vec{A}_{m+2}$  (for more details see Ref. 6). For our case, a tetrahedron defined in  $\xi$  ( $\beta, \alpha, \lambda \in \zeta$ ) where  $\zeta$  is the neighborhood of  $\lambda = 0$ , the momentum variable is the norm  $p = \left| \vec{A}_1 + \vec{A}_2 \right|$  which limits to  $A_1$  when  $\sigma$  is tented to zero. The coordinate variable  $\varphi$  is the angle between the two vectors  $\vec{A}_1 \times \vec{A}_2$  and  $\vec{A}_3 \times \vec{A}_4$  and it limits to the angle between the two unit vectors  $u_\alpha$  and  $u_\beta$  at  $\sigma = 0$ .

As we have mentioned above, the limit to the boundary must be after the quantization in order to get the correct limit (the quantum limit), which will be the quantization of the KMPS boundary. To proceed, we have first to find the KMPS in the neighborhood of the boundary, namely when  $\zeta$  surrounds  $\lambda = 0$  and then quantize it using the Planck hypothesis (BSQ condition). This procedure will



forces one to make vapid calculations. However, the calculations can be simplified using the notion of parametrized volume  $V(\sigma)$ , namely integrating  $V(\sigma)$  over classical orbits and then tending  $\sigma$  to zero. The volume in this parametrization can be defined by integrating an area  $S(\alpha(\lambda), \beta(\lambda), \lambda)$  to an arbitrary value of  $\lambda = \sigma$  such that

$$V(\sigma) = \int_{\lambda=0}^{\lambda=\sigma} S(\alpha(\lambda), \beta(\lambda), \lambda) \cdot u_\lambda d\lambda \quad (5.29)$$

where  $S(\alpha(\lambda), \beta(\lambda), \lambda) = \alpha(\lambda)\beta(\lambda)(u_\alpha \times u_\beta)$ . Considering this volume as the one of a tetrahedron, integrating over classical orbits and using the equality  $(\alpha(\lambda)\beta(\lambda)(u_\alpha \times u_\beta) + \alpha(\lambda)\sigma(u_\alpha \times u_\lambda)) \cdot u_\lambda = \alpha(\lambda)\beta(\lambda)(u_\alpha \times u_\beta) \cdot u_\lambda$  we find

$$2\pi V(\sigma) = \oint \left( \int_{\lambda=0}^{\lambda=\sigma} P(\sigma) \cdot u_\lambda d\lambda \right) d\varphi \quad (5.30)$$

where  $P(\sigma) = \alpha(\lambda)\beta(\lambda)(u_\alpha \times u_\beta) + \alpha(\lambda)\sigma(u_\alpha \times u_\lambda)$ . Notice that the norm of this vector is exactly the momentum variable in the  $\tau$ 's KMPS. Taking into account the equality  $P(\sigma) \cdot u_\lambda = |P(\sigma)| \cos \theta$  and reordering the integrations, the last equation becomes

$$2\pi V(\sigma) = \int_{\lambda=0}^{\lambda=\sigma} d\lambda \cos \theta \oint |P(\sigma)| d\varphi. \quad (5.31)$$

The term  $\cos \theta$  was put outside the integral (along  $\varphi$ ) because we have supposed first that  $u_\lambda \perp \vec{A}_1$ . Performing BSQ for the closed integral in the last equation gives

$$2\pi V(\sigma) = 2\pi h \left( n + \frac{1}{2} \right) \int_{\lambda=0}^{\lambda=\sigma} d\lambda \cos \theta \quad (5.32)$$

where  $n$  is an integer. When  $\sigma \rightarrow 0$ ,  $\cos \theta \cong 1$  and the integral  $\int_{\lambda=0}^{\lambda=\sigma} d\lambda$  reduces to  $d\lambda$ . Replacing this we find

$$V(\sigma \rightarrow 0) = h \left( n + \frac{1}{2} \right) d\lambda. \quad (5.33)$$

On the other hand,  $V(\sigma \rightarrow 0) = A_1 d\lambda$  (the factor  $\frac{1}{3}$  was dropped with the one in the right hand side of Eq. (5.33)). Substituting this in the last equation gives

$$A_1 = h \left( n + \frac{1}{2} \right). \quad (5.34)$$

The number  $n$  symbolizes the levels the Hamiltonian (the area) can take. These levels can be determined considering the fact that the area  $A_1$  is encircled by

three lengths, which give spectrum for the encircled area when these lengths are promoted into operators in an appropriate Hilbert space. But for our case, the spectrum has only one level due to the fact that the areas of the bulk tetrahedron were fixed first. This level corresponds to the chosen value of the  $SU(2)$  rotation generator, namely  $n = j$ . Switching this into the last equation gives the well-known equidistant area spectrum

$$A_1 = h \left( j + \frac{1}{2} \right). \quad (5.35)$$

In the context of KMPS, this formula was assumed in Ref. [28]. In Ref. [83], the same formula was derived by lifting the problem of angular momenta addition into the space of Schwinger's oscillators. Furthermore, it was shown in Ref. [84] that assigning the spectrum shown in this formula to the links variables in loop gravity can reproduce both the thermodynamics and the quasinormal mode properties of black holes. However, this formula has a long history starting from the Ponzano and Regge paper of Ref. [85] to the present work [83]. In comparing this with the quantization proved canonically in loop gravity [11], one can see that the quantitative agreement is extremely well in the large values of areas.

However, some aspects of this strategy are incomplete and deserve more details

- The notion of neighborhood and the limit to zero,  $\sigma \rightarrow 0$ , should not be understood mathematically, since we have performed BSQ before considering them. Instead, they can be understood physically considering the fact that for large values of areas the gap between zero volume and the minimal level of it will be considered as a differentiation (for the change in the maximum value of the coordinates  $\lambda$ , that is  $\sigma$ ). Notice that this is nicely consistent with the fact that the equidistant area spectrum does not match well the standard spectrum of the area (derived canonically in loop gravity) for small angular momentum values.
- The classical orbit that represents the minimal level for the volume can be studied using the results found in Ref. [29]. In fact, it can be considered in the case of phase spaces with no flat configurations and the corresponding volume gap can be given by  $V_{min} = c (A_1 A_2 A_3 A_4)^{\frac{1}{4}}$  where  $c$  equals to  $\frac{2}{3}$  for an odd number of levels and to  $\frac{\sqrt{2}}{3}$  for an even number.

### 5.6.4 The second strategy

According to the Planck hypothesis, Bohr-Sommerfeld orbits in phase spaces encircle symplectic areas that is  $2\pi \left(n + \frac{1}{2}\right)$  times the Planck constant. This hypothesis has been used in the first strategy (above) and the results are:

- the tetrahedron's areas are defined in phase spaces of two points bounding a symplectic lines relates these points (see Fig. 5.3),
- 
- the tetrahedron's areas are quantized equidistantly with one value in the spectrum for each area (one level for the Hamiltonian).

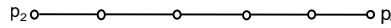


FIGURE 5.3: A symplectic line encircled (bounded) by two phase space points. The length of this line is  $2\pi \left(n + \frac{1}{2}\right)$  times the Planck constant, where (for this case)  $n = 2$ .

One may expect that these two results are related each one to the other. In fact, if we reduce the Planck hypothesis to the case when the symplectic area is one dimensional phase space, that is the length of the line bounded by the two phase space points varies in discrete steps, together with the fact that the role of the Hamiltonian generating classical orbits is played by the tetrahedron's areas then it will be an easy check to show that the spectrum of these areas is exactly that of equidistant spacing, that is

$$\oint pd\varphi = 2\pi h \left(n + \frac{1}{2}\right) = p \oint d\varphi = 2\pi A_1 \quad (5.36)$$

where we have considered the fact that  $p = A_1$  and the closed orbit as:  $p_1(A_1, \varphi_1) \rightarrow p_2(A_1, \varphi_2) \rightarrow p_1(A_1, \varphi_1)$ . Then, one can replace  $n$  by the chosen  $SU(2)$  generator as we have done above, which completes the derivation. It turns out that that this strategy is nicely consistent with studying the quantization of the tetrahedron's volume because, in this strategy, the tetrahedron's areas were considered as playing the role of Hamiltonian generating classical orbits, which fix them along these orbits.

If we want to study the dynamics of the theory using this strategy, we have to identify the phase space variables, which are two points. So, what is expected to do is that one has to support the symplectic line by a line of

coordinate and study the position of these points with respect to a chosen origin (with base of one unit vector). The two points referred to above can be determined using the relation

$$\arcsin\left(\pm\frac{2A_1}{\alpha_0\beta_0}\right) = \varphi. \quad (5.37)$$

Using the second strategy simplify very much the calculations and provides new insights into the quantization when the symplectic area is more or less than two dimensional phase space.

In summary, in this chapter, the semi classical methods into the study of the area spectrum in loop gravity using KMPS has been introduced. This quantization is nicely consistent with the quantization of the volume of space proved in Ref. [28] since it generalizes the quantization using KMPS to the case of the area of space, which gives further credibility to semi classical methods in loop gravity. The main result is summarized in Eq. (5.35), which gives an equidistant area spectrum. The key idea in this approach is not new in the field of the quantum polyhedron, in fact the author in Ref. [86] has derived a formula for the volume of pentahedron by closing it into a tetrahedron. This is somewhat analogous to our case (closing tetrahedron into an area).

## 5.7 The quantum Trihedron: Generalization

In the above derivation, the spectrum has only one level due to the fact that the tetrahedron areas were fixed first. The result was that the KMPS for the  $\tau$ 's areas are two points and the lengths of the lines relating these points in the quantization procedure vary in discrete steps. In this section, we attempt to generalize the above derivation in the sense that the Hamiltonian of our system (the area) has more than one level. To proceed, let us first establish the semiclassical ground for the quantization. This amounts to find the lengths of lines relating two phase space points in one symplectic spaces. As the momentum  $|\vec{A}_1|$  is fixed along classical orbits, those lengths are defined by the difference

$$l = \left| \arcsin\left(\frac{2\eta}{x}\right) - \arcsin\left(-\frac{2\eta}{x}\right) \right| = |f| \quad (5.38)$$

where  $x = \alpha_0\beta_0$ . Supposing  $f \succ 0$  and differentiating the two sides of the last equality gives

$$dl = d\varphi = 2d \arcsin \left( \frac{2\eta}{x} \right). \quad (5.39)$$

substituting this into Eq. (5.36) (by considering the general case for the  $\varphi$  interval) gives

$$2\eta \int_{x_1}^x d \arcsin \left( \frac{2\eta}{x} \right) = 2\pi h \left( n + \frac{1}{2} \right). \quad (5.40)$$

Performing the integration on the last equation gives

$$\eta = \frac{\pi h \left( n + \frac{1}{2} \right)}{\arcsin(\theta) - \chi} \quad (5.41)$$

where  $0 \leq \theta = \frac{2\eta}{x} \leq 2\pi$  and  $\chi = \arcsin \left( \frac{2\eta}{x_1} \right)$  such that  $\arcsin(\theta) \neq \chi$ . The computation using this formula is performed by varying  $\eta$  and taking the values that satisfy BSQ condition. If we equal the denominator to  $\pi$ , the result for  $\eta$  is an equidistant spacing spectrum (by taking  $n = j$ ).

TABLE 5.1: Comparison between the Bohr-Sommerfeld (BS) and loop gravity (LG) area spectrum. The accuracy values are computed as  $accuracy = \frac{(BS-LG)*100}{BS}$

$j_1$	Bohr-Sommerfeld	Loop gravity	Accuracy
0.5	1	$\frac{\sqrt{3}}{2}$	13.39 %
1.0	$\frac{3}{2}$	$\sqrt{2}$	5.71 %
1.5	2	$\frac{\sqrt{15}}{2}$	3.17 %
2.0	$\frac{5}{2}$	$\sqrt{6}$	2.02 %
3.0	$\frac{7}{2}$	$\sqrt{12}$	1.02 %
5.0	$\frac{11}{2}$	$\sqrt{30}$	0.41 %
8.0	$\frac{17}{2}$	$\sqrt{72}$	0.17 %
15.0	$\frac{31}{2}$	$\sqrt{240}$	0.05 %
20.0	$\frac{41}{2}$	$\sqrt{420}$	0.02 %
100.0	$\frac{201}{2}$	$\sqrt{10100}$	0.00 %
200.0	$\frac{401}{2}$	$\sqrt{40200}$	0.00 %

## Chapter 6

# The Complete Spectrum of the Volume of Space from Bohr-Sommerfeld Quantization

In this chapter, the work done in Ref. [28] is generalized (about the discreteness of the volume of space from Bohr Sommerfeld quantization concerning the node Hilbert space  $\mathcal{H}_4$  of valency four) to the case of the node Hilbert space  $\mathcal{H}_N$  with valency  $N$ . The quantization is purely semiclassical applied to grains of space, classical polyhedron, in the context of the relation between the quantum polyhedra and loop gravity addressed in Ref.[27]. The role of Hamiltonian generating classical orbits is played by the volume of space.

The fact that the volume operator acts only on nodes in spin network is considered strongly. Together with the key idea of virtual lines considered in the canonical derivation of the volume of space, the semiclassical computation of the volume of the quantum polyhedron is an immediate result.

### 6.1 The Quantum Polyhedron: The volume Spectrum

The quantization of Kapovich-Milson phase space leads to the quantum polyhedron. In the trivial case for the node Hilbert space  $\mathcal{H}_4$ , the volume of the quantum tetrahedron can be computed and studied [28]. But for  $\mathcal{H}_N$ ,  $N \geq 5$ ,

the study becomes difficult. Nevertheless, Hal Haggard has fully explored the case of  $\mathcal{H}_5$  by closing pentahedron into tetrahedron so that its volume becomes equal to the difference between two tetrahedral volumes. However, this technique does not work in general. This motivates the search for a new general technique leading to a complete computation of the volume of polyhedra. To proceed, let us first explore the key results:

- the volume of space acts only on nodes, therefore by using the virtual lines at each node we can construct new areas so that the original polyhedron becomes a set of connected tetrahedra with matching boundaries;

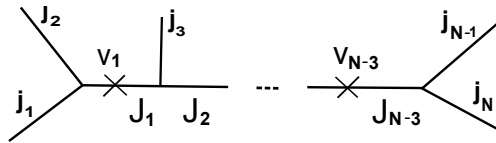


FIGURE 6.1: The network dual to polyhedra faces.

- for the node Hilbert space  $\mathcal{H}_4$  of four  $SU(2)$  rotation generators  $j, j_2, j_3$  and  $j_4$ , the semiclassical volume of tetrahedron  $V$  has a well defined action via the successful computation done by Bianchi and Haggard. We denote it as:  $V_{BH}^{v_i}$  where  $v_i$  stands for the vertex  $v$  of the index  $i$ .

It is worth to notice that:

1. the idea of introducing virtual lines is the analogous of coupling  $N$  angular momenta which is, in turn, equivalent to the simultaneous coupling of all the momenta. However, this idea is not new, it has been considered in Ref. [11] in computing the volume of space for the node Hilbert space  $\mathcal{H}_N$  with valency  $N$  (it will be clarified in the last section with some examples); and
2. this technique is not in a contradiction with Minkowski's theorem, this because that theory only concentrates on the existence and uniqueness of a polyhedron and not specifies the way it is constructed.

Let us now consider a general element of polyhedra  $\mathcal{D}_N$  with  $N$  faces (see Fig. 6.1). The number of virtual lines equals the number of nodes which is  $N - 3$ , that is  $\{v_i, i = \overline{1, (N - 3)}\}$ . We denote the generators of rotation corresponding to the virtual lines by  $J_i$ . Therefore we have:  $J_1 = j_1 + j_2, J_2 =$

$J_1 + j_3, \dots, J_{N-3} = J_{N-4} + j_{N-2}$  such that for each equality  $j_i + j_j = j_{ij}$  we have

$$j_j - j_i \leq j_{ij} \leq j_i + j_j. \quad (6.1)$$

We call  $V_{BH}^{v_i}$  the Bianchi-Haggard operator (generally we write  $V_{BH}^v$ ), which acts on the vertex  $v_i$  and gives the corresponding semiclassical spectrum. Since the action of the volume operator on any three valent vertex gives zero, the number of the possible actions on a polyhedron belonging to  $\mathcal{H}_N$  is  $(N - 3)$  and the resulted volume is the sum of all elementary volumes, that is

$$\hat{V}_{BH}^v |\chi\rangle = \sum_{i=1}^{N-3} \hat{V}_{BH}^{v_i} |v_i\rangle \quad (6.2)$$

where  $\chi$  is the network depicted in Fig. 6.1,  $v_i$  is the  $i^{\text{th}}$  node and “ $\hat{\phantom{x}}$ ” refers to the semiclassical action of the volume.

The geometric interpretation of this result is simple: suppose that we have  $N$  connected (with matching boundaries) tetrahedra, so the total volume is (clearly) the sum of all the tetrahedra volumes. The computation using this formula is performed in the framework of Ref. 3 for  $V_{BH}^v$  with respecting the condition of Eq. (6.1).

## 6.2 Examples

### 6.2.1 The three valent node $\mathcal{H}_3$ : trihedron

It is well-known that the action of the volume operator on the three valent node Hilbert space  $\mathcal{H}_3$  results zero, so how this can be understood geometrically ?

Let us take three vector areas  $\vec{A}_1, \vec{A}_2$  and  $\vec{A}_3$  such that the condition  $\sum_{i=1}^3 \vec{A}_i = 0$  holds, then it will be clear (easily) that those vectors are co-planar. Therefore the quantity  $(\vec{A}_1 \times \vec{A}_2) \cdot \vec{A}_3 = 0$ , which is corresponding action of the volume operator on three valent node Hilbert space  $\mathcal{H}_3$ .

### 6.2.2 The four valent node $\mathcal{H}_4$ : tetrahedron

This is the simplest and the elementary case. In Refs. [28, 29] the quantum study of classical tetrahedra has been performed. Two key results were



considered: (a) the volume of space is considered as playing the role of Hamiltonian generating classical orbits; and (b) the Planck hypothesis: symplectic areas vary in discrete steps and they are  $2\pi \left(n + \frac{1}{2}\right)$  times the Plank constant. The results of the semiclassical quantization, for the volume spectrum, match well the canonical quantization in loop gravity.

### 6.2.3 The five valent node $\mathcal{H}_5$ : pentahedron

In Ref. [86], Haggard fully studied the quantum pentahedron, he proved that such system is chaotic. A formula for the volume was derived by closing pentahedron into tetrahedron and taking the difference between two tetrahedral volumes. In Ref. [34], the authors provided an analysis (analytical and numerical) of the dynamics of the equifacial pentahedron. The study examines the local stability of trajectories within KMPS and addresses the chaotic property of such systems.

In such studies, the starting point is the KMPS, which is described via two pairs of canonical variables  $(p_1, \varphi_1)$  and  $(p_2, \varphi_2)$  defined by:

$$p_1 = \left| \vec{A}_1 + \vec{A}_2 \right|, \quad (6.3)$$

$$p_2 = \left| \vec{A}_1 + \vec{A}_2 + \vec{A}_3 \right|, \quad (6.4)$$

$$\varphi_1 = \text{angle} \left\{ \vec{p}_2 \times \vec{A}_2, \vec{p}_1 \times \vec{A}_3 \right\}, \quad (6.5)$$

$$\varphi_1 = \text{angle} \left\{ \vec{p}_2 \times \vec{A}_3, \vec{p}_2 \times \vec{A}_4 \right\}. \quad (6.6)$$

Let us now make use the result at Eq. 6.2. In this case, classical pentahedron, the number of nodes is two. Thus, the volume is the sum of the volumes of two tetrahedra described as it is shown in Fig. 6.1. If we denote to the Bianchi-Haggard spectrum for a node  $v_i$  with four  $SU(2)$  rotation generators  $j_1, j_2, j_3$  and  $j_4$  as  $V_{BH}^{v_i(j_1, j_2, j_3, j_4)}$ , then the volume of pentahedron  $V_{\text{pent}}$  with five  $SU(2)$  rotation generators  $j_1, j_2, j_3, j_4$  and  $j_5$  can be given as follows:

$$V_{\text{pent}} = V_{BH}^{v_1(j_1, j_2, j_3, j_4)} + V_{BH}^{v_2(j_1, j_3, j_4, j_5)} \quad (6.7)$$

The physical interpretation of this result is simple: the volume  $V_{\text{pent}}$  is the sum of the volumes of two connected tetrahedra (with a face). Notice that the

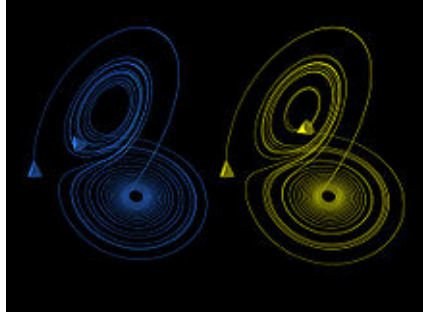


FIGURE 6.2: The Lorenz attractor displays chaotic behavior. These two plots demonstrate sensitive dependence on initial conditions within the region of phase space occupied by the attractor.

connection is valid since the condition of *matching boundaries* is respected (the two tetrahedra sharing a common area, that is  $|\vec{A}_3|$ ).

### 6.2.3.1 The chaotic behavior

Edward Lorenz summarized the notion of chaos as follows *chaos: when the present determines the future, but the approximate present does not approximately determine the future*. The notion of chaos for pentahedron has been discussed in Refs. [34, 86]. Here, we show an independent road to that fact. We have seen from the last subsection that the volume of the original pentahedron  $V_{\text{pent}}$  is the sum of the volumes of two tetrahedra  $V_{\text{tet}_1}$  and  $V_{\text{tet}_2}$ . Furthermore, notice that the two pairs  $(p_1, \varphi_1)$  and  $(p_2, \varphi_2)$  are associated with  $V_{\text{tet}_1}$  and  $V_{\text{tet}_2}$  respectively (note that  $p_2 = |\vec{A}_1 + \vec{A}_2 + \vec{A}_3| = |\vec{A}_4 + \vec{A}_5|$ ). This means that the two volumes are constants along classical orbits of the corresponding pair of the phase space.

Now, for simplicity let us suppose that  $\vec{p}_1 \perp \vec{p}_2$ . So, if we pick up a level for  $V_{\text{tet}_1}$  and another for  $V_{\text{tet}_2}$  then you can visualize (geometrically) that we have two orbits span a sphere. That is, one can move arbitrarily on the sphere provided that this movement has a closed orbital projections on the planes defined by  $(p_1, \varphi_1)$  and  $(p_2, \varphi_2)$ . The orbits on the sphere (for  $V_{\text{pent}}$ ) are not closed necessarily; this means that the volume  $V_{\text{pent}}$  presents a clear chaotic behavior. Notice that the volume  $V_{\text{pent}}$  is constant on 3d spheres surfaces defined by picking up two levels for  $V_{\text{tet}_1}$  and  $V_{\text{tet}_2}$ , but the latter are not constant separately (on the spheres surfaces). Fig 6.2, above, the Lorenz attractor, displays a chaotic behavior studied by Lorenz.

# Chapter 7

## The Quantum Pentahedra

Recently [86], it has been shown that closing a pentahedron into tetrahedron allows to explicitly find the volume of the pentahedron. This amounts to consider a map  $\pi_{\text{volume}} : \mathcal{P}_5 \mapsto \mathcal{P}_4 \times \mathcal{P}_4$  from the space of shapes of the pentahedron into the spaces of shapes of the resulted two tetrahedra.

In this chapter, we provide an alternative approach. Two key results are considered in doing so: (a) the fact that the volume operator acts only on nodes in spin network and (b) the idea of virtual lines considered in the canonical derivation of the volume in Ref. [11]. The volume spectrum for pentahedron, we find, has a very similar form to the one found by Hal Haggard [86], but with a rich structure in which the earlier Bohr's model of atoms gets arisen.

### 7.1 The Haggard's Rescaling Reconstruction

The quantization of Kapovich-Milson phase space leads to the quantum polyhedron. In the trivial case for the node Hilbert space  $\mathcal{H}_4$ , the volume of the quantum tetrahedron can be computed and studied [28, 29]. But for  $\mathcal{H}_N, N \geq 5$ , the semiclassical computation of the volume becomes difficult. Nevertheless, the author in Ref. [86] fully explored the case of  $\mathcal{H}_5$  by closing pentahedron into tetrahedron so that the tetrahedral-volume is reproduced via the difference of tetrahedral-volumes. Roughly speaking, Let us consider a pentahedron  $P \in \mathcal{P}_5$ , which can be closed into a tetrahedron  $T_1 \in \mathcal{P}_4$  (as

it was done in Ref. [86], see Fig. 1 in it). The Haggard's rescaling reconstruction is the step from

$$\vec{A}_1 + \vec{A}_2 + \vec{A}_3 + \vec{A}_4 + \vec{A}_5 = 0 \quad (7.1)$$

to

$$\alpha\vec{A}_1 + \beta\vec{A}_2 + \gamma\vec{A}_3 + \vec{A}_4 = 0 \quad (7.2)$$

where  $\{\vec{A}\}$  are the non-coplanar vectors areas of P. The main result within this rescaling has been the formula for the P's volume

$$V_{\text{pent}} = \frac{\sqrt{2}}{3} \left( \sqrt{\alpha\beta\gamma} - \sqrt{\bar{\alpha}\bar{\beta}\bar{\gamma}} \right) \sqrt{W_{123}} \quad (7.3)$$

where  $W_{ijk} = \vec{A}_i \cdot (\vec{A}_j \times \vec{A}_k)$ ,  $\alpha = -\frac{W_{234}}{W_{123}}$ ,  $\beta = -\frac{W_{134}}{W_{123}}$ ,  $\gamma = -\frac{W_{124}}{W_{123}}$  and  $\bar{x} = x - 1$ ;  $x = \alpha, \beta, \gamma$ . This construction allows to define  $\pi_{\text{volume}}$  as

$$\pi_{\text{volume}} : \quad \mathcal{P}_5 \quad \rightarrow \quad \mathcal{P}_4 \times \mathcal{P}_4 \quad (7.4)$$

$$\text{Eq. (3)} \quad \rightarrow \quad \text{Eq. (4)}. \quad (7.5)$$

where  $\mathcal{P}_4 \times \mathcal{P}_4$  correspond to  $T_1$  and  $T_2$  such that  $T_2$  is the tetrahedron that close P into  $T_1$ . The P's volume is taken as the Hamiltonian, generating classical orbits, of the P's system.

## 7.2 An alternative approach to the pentahedron volume

Two technical steps are considered for the present task: (a) splitting the P's graph into two connected tetrahedral graphs via virtual lines (as it was done in Ref. [11]) and (b) taking into account the fact that the volume operator acts only on nodes in spin network. This amounts to explore a graph with two virtual lines  $J_1, J_2$  and two four valent vertices  $v_1$  and  $v_2$ . See Fig. 7.1.

Considering the statement at (b) leads us to write the volume of P as

$$V_{\text{pent}} = \frac{\sqrt{2}}{3} (V_{v_1}(j_1, j_2, j_3, J_2) + V_{v_2}(J_1, j_3, j_4, j_5)), \quad (7.6)$$

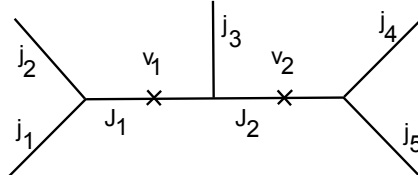


FIGURE 7.1: The P's graph as two connected tetrahedral graphs, which are dual to two connected tetrahedra  $T_1$  and  $T_2$  by the area  $|\vec{A}_3|$  dual to  $j_3$

therefore we write

$$V_{\text{pent}} = \frac{\sqrt{2}}{3} \left( \sqrt{W_{123}} + \sqrt{W_{345}} \right) \quad (7.7)$$

$$= \frac{\sqrt{2}}{3} (1 + \eta) \sqrt{W_{123}} \quad (7.8)$$

where  $\eta = \frac{\sqrt{W_{345}}}{\sqrt{W_{123}}}$ . Notice that this formula is somewhat analogous to the one of Haggard defined in Eq. 7.3, but with an additional constraint due to the existence of a shared area  $|\vec{A}_3|$  connecting the two tetrahedra. In fact even this constraint, it has a correspondence in the Haggard's rescaling reconstruction; if we denote the areas of the dashed tetrahedron (see Fig. 1 in Ref. [86]), that is  $T_2$ , by  $\vec{A}_1, \vec{A}_2, \vec{A}_3, \vec{A}_4$ , one can write

$$\vec{A}_1 + \vec{A}_2 + \vec{A}_3 + \vec{A}_1 + \vec{A}_2 + \vec{A}_3 + \vec{A}_4 = 0. \quad (7.9)$$

where  $\{\vec{A}_i, i = \overline{1,4}\}$  stand for the P's areas.

It is to be noted that: the two tetrahedra  $T_1$  and  $T_2$  are constructed by considering the coupling in Fig. 7.1. Thus, one may wonder that these tetrahedra present some possible interference. However, it has been argued [1–4] that the volume and area of space in loop quantum gravity should not naively be thought as something to manipulate directly, but they are understood the way they act (because the spacetime is not defined in a spacetime, it is spacetime itself). Furthermore, we have seen that the volume is taken as the Hamiltonian generating classical orbits, thus it has the role of energy and we know that the energy can be associated with a density, so the fact that tetrahedra are interfered is not something to worry about. Notice that even in the Hal Haggard's rescaling reconstruction this interference is taking place in the sense that

$$T_{1\text{space}} \cap T_{2\text{space}} = T_{1\text{space}} \quad (7.10)$$

where  $\{T_{j_{\text{space}}}, j = 1, 2\}$  refer to the space of points covered by the convex hull of the corresponding tetrahedra.

### 7.3 The physical interpretation

Our interpretation to the findings is based on an observation and a technical tool:

1. in Ref. [59], it has been shown that the areas of tetrahedron can be studied and quantized using KMPS and BSQ, i.e. they have orbits along which they are constant. Let us denote these orbits by ;
2. we represent the areas of polyhedra via points-like particles on phase spaces. This choice is motivated by the fact that the areas are studied in loop gravity as entire objects with specific levels. On the other hand, the change in the configurations (over orbit-configurations) does not affect the Hamiltonian.

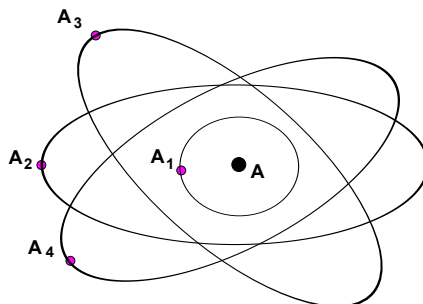


FIGURE 7.2: The quantum tetrahedron depicted on phase spaces. Its areas are presented by points-like particles moving on the corresponding phase-space-orbits. The big black point refer to the area  $|\vec{A}| = |\vec{A}_1 + \vec{A}_2| = |\vec{A}_3 + \vec{A}_4|$ , which represents, in turn, a point-like particle playing the role of the tetrahedron's noyau.

Via the above two idems, the quantum tetrahedra can be depicted as in Fig 7.2.

For our case, the quantum pentahedron, we have two connected tetrahedra. Thus if we denote the volume-orbits of  $T_1$  by  $\tau_1$  and similarly for  $T_2$  by  $\tau_2$ , then the quantum pentahedron can be depicted as in Fig. 7.3. Note that in this depiction, we have considered the simplest case; the the volumes of the two connected tetrahedra are constant along an orbit  $o \in P$ . The general case is not constrained with this.

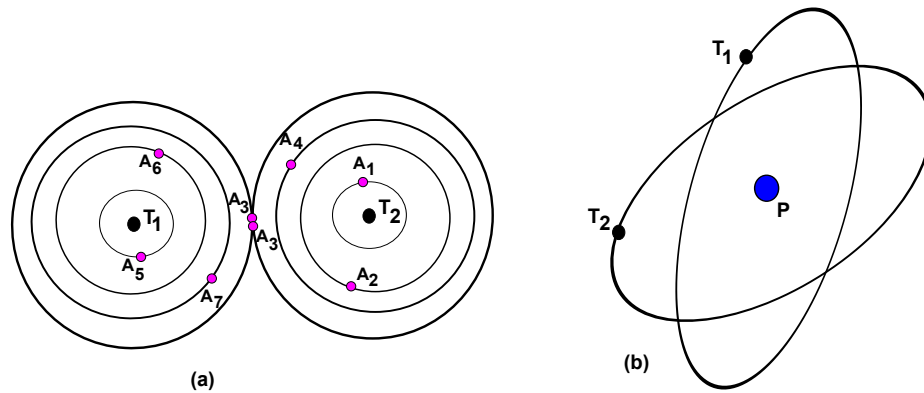


FIGURE 7.3: (a) Two connected tetrahedra by the area  $|\vec{A}_3|$ . The illustration is intended to be considered to imagine the real case (orbits in 3d space). (b) The two tetrahedral noyaux of  $T_1$  and  $T_2$  moving on the corresponding phase-space-orbits around a common center called the pentahedron's noyau. The big blue point refer to the area  $|\vec{A}_P|$  of P defined by  $|\vec{A}_P| = |\vec{A}_1 + \vec{A}_2 + \vec{A}_3| = |\vec{A}_4 + \vec{A}_5 + \vec{A}_3|$ , which is playing the role of the pentahedron's noyau moving long the corresponding phase-space-orbits of the pentahedron.

The results shown in this chapter show a remarkable similarity between the structure of spacetime and the one of ordinary matter. This can be understood in the sense that in ordinary matter the phase space variables are exactly the spacetime coordinates (in the Bohr model of atoms, the radial variables  $r$  and the angle  $\theta$  of an electron's orbit can be replaced in the spherical coordinates). While in loop gravity, some reconsiderations are considered because the fact that the area variables are the natural variables in loop gravity, see for instance Ref. [1, 2].

# Chapter 8

## Regge and Twisted Geometries in Loop Gravity

In practical dealing with loop gravity people usually restrict the attention to a finite number of gravitational field variables [1–3, 87], allowing to capture the physics of appropriate regimes. This restriction called *truncation*, it is defined via states supported by a graph  $\Gamma$  in the Hilbert space  $\mathcal{H}_\Gamma$ . The truncation may reflect the Regge geometries [88] or (more generally) the twisted geometries [89, 90]. The computation of the holonomy-Flux variables over a Regge-truncation of general relativity (GR) leads to twisted geometries [87], but does (generally) work for a twisted-truncation of GR?

The trial to answer the question leads to generalize the work done by Rovelli and Speziale of Ref. [87] to the case where the matching in the area-configuration does not hold. More explicitly, the question leads us to compute the extrinsic curvature across a face connecting two tetrahedra with no matching in the area-configuration.

### 8.1 Regge and twisted geometries

In Ref. [89], a geometric parametrisation of  $SU(2)$  phase space is studied. In Ref. [87], the relation of this constructions to loop quantum gravity is discussed. In this section, we summarize the relevant points to the present work.



The essential results to be noted here is that the computation of the holonomy and the flux of the electric field in a given 4d Regge geometry reproduces exactly the canonical transformation of the parametrisation studied in Ref. [89]. To proceed into the details, let us consider a graph  $\Gamma$  with  $l$  links and  $n$  nodes determining 3d discrete quantum geometry. The study is bridged to semiclassical description via coherent states. The phase space of the theory is the one of Ashtekar given by the pair  $(E_i^a(x), A_a^i(x))$  where  $E_i^a(x)$  and  $A_a^i(x)$  are the electric field and connection respectively. The graph  $\Gamma$  supports states belonging to the Hilbert space  $\mathcal{H}_\Gamma$  which corresponds to a truncation of the theory. Here,  $\Gamma$  is constructed via  $L$  copies of  $SU(2)$ , that is we have  $SU(2)^L$ , and the holonomy plays the role of coordinates and it is invariant under gauge transformations as  $U_l \rightarrow V_{s(l)} U_l V_{t(l)}^{-1}$ , such that  $V, U \in SU(2)$  and  $s(l), t(l)$  are the source and the target node of the link  $l$  respectively. With this, the phase space becomes  $(U_l, X_l)$  where  $X$  are generators of  $SU(2)$  rotations.

Twisted geometries are a class of discrete metric spaces with the following set of variables

$$\left( N_l, \tilde{N}_l, j_l, \xi_l \right) \in P_l \equiv S_2 \times S_2 \times R \times S_1 \quad (8.1)$$

for each link  $l$  of two normals  $N_l$  and  $\tilde{N}_l$  defined in the two frames that share the face dual to the link  $l$  of area  $|j|$  where  $\xi$  is a quantity related to the extrinsic curvature at  $l$ . The task of Ref. [87] was to explore the following correspondence

$$X = jn\tau_3\tilde{n}^{-1}, \quad (8.2)$$

$$U = ne^{\xi\tau_3}\tilde{n}^{-1} \quad (8.3)$$

where  $X = X^i\tau_i \in su(2)$ ,  $\tau_i$  ( $i = \overline{1,3}$ ) are the Pauli matrices multiplied by  $-i/2$  and  $n, \tilde{n} \in SU(2)$ . To proceed, let us consider a 4d Regge manifold (which is built via glued flat four-simplices with matching geometry) and an initial hypersurface data  $\Sigma$  in it.  $\Sigma$  can be seen as a collection of tetrahedra endowed with intrinsic (on the edges) and extrinsic (on the triangles) curvatures. Across a face  $f$  in  $\Sigma$ , the 4d normal to  $\Sigma$  changes and defines a quantity called the extrinsic curvature given by (see Ref. [87] for more

details)

$$k_{ab} = \theta \int_f \delta^3(x, f(\sigma)) d^2\sigma = \theta N_a N_b \quad (8.4)$$

where  $\theta$  is the dihedral angle between the 4d normals to the two tetrahedra at  $f$  and  $N$  is the normal to the face  $f$ . In this context, the holonomy-flux variables can be computed via

$$X_l^i = \int_f E^{ai} N_a d^2\sigma, \quad (8.5)$$

$$U_l = \mathcal{P} \exp \int_l dl^a (\Gamma_a^i + \gamma e_a^i k_{ab}) \tau_i \quad (8.6)$$

where  $E^{ai}$  is the Ashtekar's electric field,  $\Gamma_a^i + \gamma e_a^i k_{ab}$  is the Ashtekar-Barbero connection and the notation  $\mathcal{P}$  refers to the path ordering along  $l$ . After some calculations (with a chosen gauge), one can get

$$X_l^i = j N^i, \quad (8.7)$$

$$U_l = n e^{(\gamma\theta - \alpha)\tau_3} \tilde{n}^{-1} \quad (8.8)$$

where  $N^i = e^{ia} N_a$  and  $\alpha$  is an angle of rotation between the two frames sharing the face  $f$ . The last two equations map the holonomy-flux variables into twisted geometry defined in Eqs. 8.2 and 8.2.

The above analysis handles the case when the areas of the two connected tetrahedra sharing the face  $f$  have the same configuration. However, the general case is not constrained with this matching and it extends more generally in the sense that the configuration has not to be generally matched, which extends the geometry to be not (generally) the Regge one.

## 8.2 Twisted Geometries from Holonomy-Flux variables computation

In Ref. [87], it has been shown that the explicit computation of the holonomy-flux variables over a Regge-truncation of GR leads to twisted geometries. Here, we show that we get the same result, but with a twisted-truncation. To proceed, let us start computing the extrinsic curvature across a shared-face (with no matching in the area-configuration, of course) in two connected tetrahedra, see Fig. 8.1. The 4d normal to  $\Sigma$  varies only across the shared-

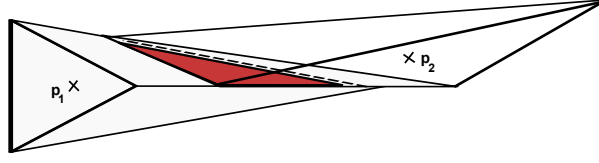


FIGURE 8.1: Two connected tetrahedra by an area with no matching in the area-configuration. The two points  $p_1$  and  $p_2$  refer to the general location inside the tetrahedra (not single points)

face  $f$  (of direction  $N_a$ ) and it is clear that its variation is orthogonal to this face (for more details see Ref. [87]), therefore the extrinsic curvature defined across  $f$  takes the form

$$K_{ab} = \theta \int_{f_t} \delta^3(x, f(\sigma_t)) d^2\sigma_t = \theta N_a N_b \quad (8.9)$$

where we have added the index  $t$  to refer to the no matching in the area-configuration of the two connected tetrahedra (i.e. we have a twisted-truncation). The quantity  $\theta$  is defined to be the dihedral angle between the 4d normals to the two tetrahedra at  $f_t$ .

The problem with this construction is that we have no idea about the face  $f_t$  because of the fact that its configuration varies at each point on the orbits associated with the volumes of the two connected tetrahedra (the shared-face should not be thought as corresponding to a fixed area-configuration). The trial to overcome this problem leads us to explore the fact that the tetrahedral edges corresponding to the shared-area allows to identify the set of points, say  $\mathcal{X}$ , that is bounded by the shared-face edges. This set is expected naturally to include the change in the configuration at each point  $p$  of the Hamiltonians-orbits of the system. The key idea to go further in this, is the fact that the tetrahedral edges can be determined explicitly via the areas of the two tetrahedra. Let us denote the areas-vectors of the first tetrahedron by  $A_1, A_2, A_3, A_4$  and the second by  $\acute{A}_1, \acute{A}_2, \acute{A}_3, \acute{A}_4$ , suppose that the two connected areas are  $A_1$  and  $\acute{A}_1$ , denote the set of points  $p \in A_1$  by  $\mathcal{X}_1$  and  $p \in \acute{A}_1$  by  $\mathcal{X}_\acute{1}$ . Therefore, we have

$$\mathcal{X} = \mathcal{X}_1 \cap \mathcal{X}_\acute{1}. \quad (8.10)$$

Furthermore, we determine two pairs of two edges  $(e_1, e_2)$  and  $(\acute{e}_1, \acute{e}_2)$  bounding  $A_1$  and  $\acute{A}_1$  respectively using the vectorial product of the tetrahedral

areas-vectors, i.e.

$$e_1 = \alpha A_1 \times A_2, \quad (8.11)$$

$$e_2 = \beta A_1 \times A_3, \quad (8.12)$$

$$\acute{e}_1 = \acute{\alpha} \acute{A}_1 \times \acute{A}_2, \quad (8.13)$$

$$\acute{e}_2 = \acute{\beta} \acute{A}_1 \times \acute{A}_3 \quad (8.14)$$

where  $\alpha, \beta, \acute{\alpha}$  and  $\acute{\beta}$  are functions not depending on the configurations of the two tetrahedra. They are introduced to guaranty that the quantities  $|e_1|, |e_2|, |\acute{e}_1|$  and  $|\acute{e}_2|$  have the lengths of the tetrahedral edges, and can be given explicitly via

$$\alpha = \beta = \frac{1}{Q}, \quad (8.15)$$

$$\acute{\alpha} = \acute{\beta} = \frac{1}{\acute{Q}} \quad (8.16)$$

where  $Q$  and  $\acute{Q}$  stand for the tetrahedral volumes of the two connected system.

Now, let us introduce two pairs of coordinates  $(x_1, x_2)$  and  $(\acute{x}_1, \acute{x}_2)$  with the bases defined by the two pairs  $(e_1, e_2)$  and  $(\acute{e}_1, \acute{e}_2)$  respectively, therefore one has:

$$0 \leq x_1 \leq (x_1)_{max} = 1, \quad (8.17)$$

$$0 \leq x_2 \leq (x_2)_{max} = 1, \quad (8.18)$$

$$0 \leq \acute{x}_1 \leq (\acute{x}_1)_{max} = 1, \quad (8.19)$$

$$0 \leq \acute{x}_2 \leq (\acute{x}_2)_{max} = 1. \quad (8.20)$$

Notice that the manifold, say  $\mathcal{M}$ , constructed by the coordinates  $(x_1, x_2; \acute{x}_1, \acute{x}_2)$  is four dimensional exactly the same as the dimension of the phase space of the theory (two connected tetrahedra). This means that the manifold in which the extrinsic curvature is defined (in a twisted geometry) locally has the dimension of the corresponding phase space. Furthermore, one can see that the doublets  $\{(x_1, x_2)\}$  and  $\{(\acute{x}_1, \acute{x}_2)\}$  reproduce  $\mathcal{X}_1$  and  $\mathcal{X}_\acute{1}$  as  $\mathcal{X}_1 \equiv \{(x_1, x_2)\}$  and  $\mathcal{X}_\acute{1} \equiv \{(\acute{x}_1, \acute{x}_2)\}$ .

Via the above analysis, the face  $f_t$  across which the extrinsic curvature is defined can be defined very-well via the relation

$$f_t \equiv \mathcal{X}. \quad (8.21)$$

The holonomy-flux variables can be computed in the same way as it was done in section 2, but by replacing  $f$  with  $f_t$ .

The Regge geometries can be obtained by imposing the following additional constraints

$$\mathcal{X} = \mathcal{X}_1 = \mathcal{X}_1. \quad (8.22)$$

This results discussed in this chapter show how the Regge and twisted geometries are related. Furthermore, they reflect the generality of the twisted geometries and the particularity of the Regge ones. Moreover, they can have important applications in the quantum polyhedra [27–29].

# Chapter 9

## Regge and Twisted Geometries in Schwarzschild Spacetime

In testing general theory of relativity, people usually focus on Schwarzschild space-time. For this reason, the study of quantum gravity in this field of space takes an important interest hoping to find tests for loop gravity.

Thus, it is natural to try to find out a mechanism by which the spacetime manifold coordinates are discretized, in particular Schwarzschild's manifold coordinates. A moment of reflection leads to explore the results derived in Refs. [87, 91]. In fact, in Ref. [87], the authors derived an elegant and nice relation between Regge and twisted geometries. This relation is considered in dealing with the extrinsic curvature and computing the holonomy along Schwarzschild geodesics; in Ref. [91], the extrinsic curvature in Schwarzschild spacetime is computed (in part). This result is considered in constructing the quantum geometry for Schwarzschild spacetime.

### 9.1 The quantum Schwarzschild spacetime

What is the possible graph for Schwarzschild spacetime? The trial to answer this question leads us to a specific discretization of the Schwarzschild spacetime manifold coordinates. This discretization is the center problem of the present paper.

Let us first discuss some results in the literature. In Ref. [92], some useful discussion about the possible graph for a Schwarzschild spacetime is given.

The discussion motivated the choice of what is known as *the wheel graph*. In Ref. [93], the author motivated the choice that the graph has to be structured with the maximum number of continuum points, this amounts to add *non-radial edges* (see for instance Ref. [92]). These results are very useful heuristic ideas, but some modifications are needed in order that the above question get answered correctly.

The problem with the above graphs is that: (a) they are constructed before exploring the mathematical structure of the holonomy-flux variables (via Schwarzschild metric) and (b) the fact that the area of space is the natural variable in loop gravity (see for instance [1–3]) is not considered seriously; in fact, the infinitesimal calculation (as it looks in the large scale) has to be based on this variable. Thus, one is motivated to search for a new graph resolving the above problems provided that it is still of spherical symmetry. The fact that the holonomy-flux variables can be computed explicitly is the key result to construct the correct graph. To see how does this work, we follow the following two steps:

1. we compute the holonomy-flux variables via Schwarzschild metric. This step is the task done in Ref. [91]. The results are

$$K_a^i = -\frac{\partial}{\partial R} e_a^i \quad (9.1)$$

where  $K_a^i = \frac{1}{\sqrt{\det(E)}} K_{ab} E_j^b \delta^{ij}$ ,  $K_{ab} = \frac{1}{2} \partial_\tau q_{ab}$  and  $E_i^a = \frac{1}{2} \epsilon^{abc} \epsilon_{ijk} e_b^j e_c^k$ . The pair  $(R, \tau)$  (Lemaitre coordinates) is the transformed Schwarzschild pair  $(r, t)$  in order that the studied slice  $\Sigma$  becomes *constant  $\tau$  slices*. Let us denote the manifold constructed by Lemaitre coordinates by  $\mathcal{L}$ . In this manifold, we attempt to interpret  $\{E_j^b\}$  geometrically. One can see that this set, let us denote it by  $\mathcal{E}$ , is of three areas orthogonal at any point of spacetime, so one can add the closure area face and get the following interpretation: *constructs at any point of spacetime a tetrahedron* (to understand how does this work, see Ref. [87]; Through the perspective in it, you can relate the extrinsic curvature with this structure),

2. we discretize the coordinates of  $\mathcal{L}$  by considering the fact that the area of space is the natural variable in loop gravity and the infinitesimal calculations should be based on this variable. This discretization can

be performed as follows:

$$E_1^R = \rho^2 \sin \theta = j_R + \frac{1}{2}, \quad (9.2)$$

$$E_2^\theta = \sqrt{r_s \rho} \sin \theta = j_\theta + \frac{1}{2}, \quad (9.3)$$

$$E_3^\phi = \sqrt{r_s \rho} = j_\phi + \frac{1}{2} \quad (9.4)$$

where  $r_s$  is the Schwarzschild constant radius,  $j_R, j_\theta, j_\phi = \frac{1}{2}, 1, \dots$  (we have considered the large values in which one can approximate by the equidistant spacing spectra) and  $\rho = [\frac{3}{2}(R - \tau)]^{\frac{2}{3}} r_s^{\frac{1}{3}}$ . These equations allow to vary the coordinates of  $\mathcal{L}$  freely provided that the area of space is the natural variable to be dealt with infinitesimally.

This construction opens a central question, what is the right geometry that can be assigned to the Schwarzschild spacetime graph. In order that this question get answered correctly, we first discuss the relation between Schwarzschild geodesics and the extrinsic curvature. Throughout the above construction and considering the results in Ref. [87], one can see that: (a) the jumping in moving along a Schwarzschild geodesic does not generally preserve the matching in the configurations of the shared areas separating two tetrahedra of a jump. This result reflects the statement: *Regge geometries are not generally valid and they only correspond to some specific geodesics*; the general case requires more general geometries such as *twisted geometries*.

Fig. 9.1 displays a visualization to the way gravity affects a test particle; it provides a way to imagine the structure of spacetime in the presence of matter. The source of gravity is presented as a huge node Hilbert space  $\mathcal{H}_N$  of valency  $N$ ; the test particle presents a small spherical symmetry Schwarzschild spacetime graph. A visualization to the way gravity affects a test particle is given: the huge node Hilbert space (gravity source) affects the configuration of the areas and the latter are connected with the test particle, which in turn affect the test particle. In order to be familiar with the Schwarzschild spacetime graph and the picture about this construction becomes more clear, we provide a computation of the holonomy along Schwarzschild geodesics. In Ref. [87], the computation of the extrinsic curvature is performed only for two adjacent tetrahedra. This computation for a Schwarzschild geodesic between two points  $p_1$  and  $p_2$  looks as an elementary extrinsic curvature. This is can be considered in the following sense: if we have a test particle



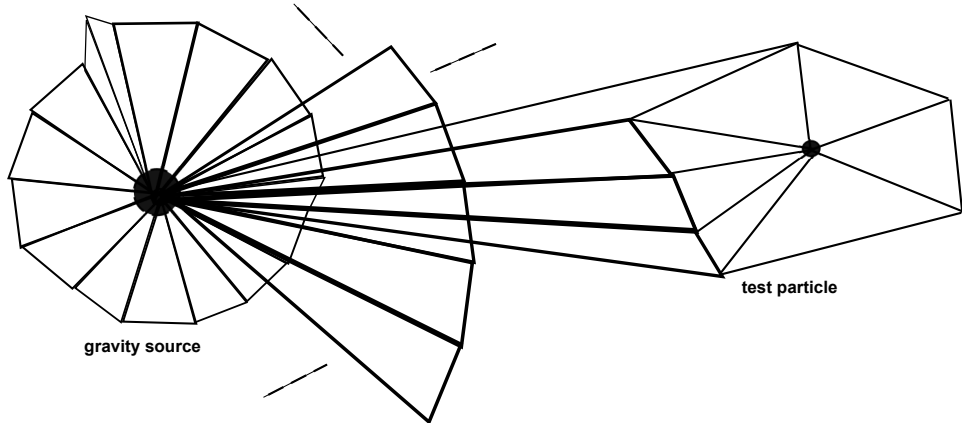


FIGURE 9.1: A source of gravity (the big ball) and test particle (the small ball) embedded in a 2d graph. The illustration is intended to be considered to imagine the real case which is in three dimensional space: each triangle is replaced by a tetrahedron and the 2d graph becomes 3d one. The dashed lines refer to the presence of additional structures not presented.

moving along a Schwarzschild geodesic, then it will be at any time located in a given volume which is the integration of elementary volumes, and the latter are having different 4d vectors (perpendicular to  $\Sigma$ ) at any point of the geodesic. This means that the test particle will get a series of actions of curvatures (along the geodesic) and the total action on the particle is the sum of all the actions or simply the integration. Therefore, between  $p_1$  and  $p_2$  in a Schwarzschild geodesic, the total holonomy is defined as:  $U_T = U_{l_1} U_{l_2} \cdots U_{l_n} = n_{l_1} e^{(\gamma \Theta_{l_1} - \alpha_{l_1}) \tau_3 \tilde{n}_{l_1}^{-1}} \cdot n_{l_2} e^{(\gamma \Theta_{l_2} - \alpha_{l_2}) \tau_3 \tilde{n}_{l_2}^{-1}} \cdots n_{l_n} e^{(\gamma \Theta_{l_n} - \alpha_{l_n}) \tau_3 \tilde{n}_{l_n}^{-1}}$ . Thus, one has to get

$$U_T = n_{l_1} e^{(\gamma \sum_{i=1}^n \Theta_{l_i} - \sum_{i=1}^n \alpha_{l_i}) \tau_3 \tilde{n}_{l_n}^{-1}} \quad (9.5)$$

where  $n$  is the number of jumps recorded by the test particle between  $p_1$  and  $p_2$ . Note that we have considered a geodesic compatible with Regge geometries and fixed  $\theta$  to be  $\frac{\pi}{2}$ ; the holonomy is computed along a geodesic parametrized in the plane  $(R, \phi)$ .

As we have discussed, in the large scale each quantity in the sum corresponds to an elementary object, which amounts to replace the sum with an integration, that is we have

$$U_T = n_{l_1} e^{(\gamma \int \Theta_{l_i} - \int \alpha_{l_i}) \tau_3 \tilde{n}_{l_n}^{-1}}. \quad (9.6)$$

Now, let us make use the result at Eq. 9.1 . Remind that we have discretized

$\mathcal{L}$ 's coordinates, and at each point of Schwarzschild spacetime the curvature computed at Eq. 9.1 corresponds to a value of  $\{\theta_{l_i}\}$ . This leads us to write

$$U_T = n_{l_1} e^{(\gamma \int (-\frac{\partial}{\partial R} e_\phi^3) - \int \alpha_{l_i}) \tau_3} \tilde{n}_{l_n}^{-1}. \quad (9.7)$$

integrating over  $R$  and taking the rotation between the two frames (the initial the the final tetrahedron) as  $\int \alpha_{l_i} = \Xi$ , we get

$$U_T = n_{l_1} e^{(-\gamma \rho - \Xi) \tau_3} \tilde{n}_{l_n}^{-1}. \quad (9.8)$$

This gives the total parallel transport along the geodesic.

The electric field  $X$  is a vectorial quantity, its total can be seen as the sum of all its elementary vectors along the geodesic, by considering the continuous variation of  $\rho$  between the two points  $p_1$  and  $p_2$  and taking the values that satisfy its discrete aspect.

The above computation is defined in the Lemaitre manifold, so one has to consider the following transformations to get measurable quantities in the Schwarzschild manifold:

$$d\tau = dt + \sqrt{\frac{r_s}{r}} \frac{1}{1 - \frac{r_s}{r}} dr, \quad (9.9)$$

$$dR = dt + \sqrt{\frac{r}{r_s}} \frac{1}{1 - \frac{r_s}{r}} dr \quad (9.10)$$

The results of this chapter provide a discretization for Schwarzschild manifold, which can be considered in searching for tests for loop gravity. Furthermore, they provide a truncation of general theory of relativity closely related to the full theory since the Schwarzschild manifold is the full space in the case of spherical symmetry. Moreover, the findings can have important applications in developing semiclassical methods in loop gravity [27] for Schwarzschild spacetime.

# Chapter 10

## Space Density from Loop gravity

In this chapter, we collect some results recently obtained from Refs. [64, 87, 91] in a consistent way, and then try to find out a new property for spacetime called *space density*. The fact that (in the quantum polyhedra) the volume of space  $V_s$  is playing the role of the Hamiltonian generating classical orbits, it has to be considered seriously:  $V_s$  should not be taken just as an abstract mathematical notion, but as a physical quantity representing the energy.

### 10.1 Space Density

In the context of the results of Refs. [64, 87, 91], let us first start with a simple example (for simplicity). Consider three tetrahedra  $T_1, T_2$  and  $T_3$  with a common corner  $c$ . We denote by  $\{T_{j_{\text{space}}}, j = \overline{1,3}\}$  the spaces of points covered by the convex hulls of the tetrahedra  $\{T_j, j = \overline{1,3}\}$ . Fig. ?? displays three different regions  $R_1, R_2$  and  $R_3$  defined by

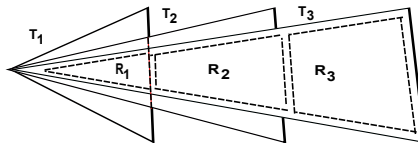


FIGURE 10.1: Three tetrahedra with a common corner. This illustrates the real case (three dimensional space); the triangles are replaced by tetrahedra and the 2d areas becomes 3d regions.

$$R_1 = T_{1\text{space}} \cap T_{2\text{space}} \cap T_{3\text{space}}, \quad (10.1)$$

$$R_2 = T_{2\text{space}} \cap T_{3\text{space}}, \quad (10.2)$$

$$R_3 = T_{3\text{space}}. \quad (10.3)$$

But the three tetrahedra  $\{T_j, j = \overline{1,3}\}$  have the common corner  $c$ , thus any point  $p \in R_1$  presents a degeneracy  $g = 3$ , i.e. it reflects the position in  $T_1, T_2$  and  $T_3$ . If we define a quantity called space density  $\mathcal{D}_R$  for a region  $R$  as the number of intersections recorded on this region, and gauge the space density of separate tetrahedron (no intersection recorded on its region) to be one, it is then clear to write

$$\mathcal{D}_{R_1} = 3, \quad (10.4)$$

$$\mathcal{D}_{R_2} = 2, \quad (10.5)$$

$$\mathcal{D}_{R_3} = 1. \quad (10.6)$$

It is worth to note that the space density discussed here is not an abstract mathematical visualization but a deep property characterizing the space-time. Furthermore, it was shown that (in the quantum polyhedra [27–29]) taking the volume of tetrahedra as playing the role of the Hamiltonian generating classical orbits reproduces the right spectrum of the volume found in loop gravity. Even canonically [44–46], it was shown that the Hamiltonian constraints affect the spacetime structure by adding a quanta of space, or simply a volume. Thus, a density for space is not something to worry about, it is like assigning a density for the energy.

Let us now generalize the idea to the Schwarzschild spacetime graph. Because of the complexity of the construction, we restrict our computation of space density to the contributions of the tetrahedra  $\{T_i, i = \overline{1,n}\}$  along the  $R$ -line coordinate and take  $\theta = \frac{\pi}{2}$  (in the Lamaiter coordinates, of course). First, we suppose that the gravitational field, say  $\mathcal{F}$ , of our system  $\mathcal{F} \cong 0$  at  $\rho = \rho_{\max}$ , therefore it is possible to find  $n$  as

$$n = 2(j_R)_{\max} + 1 \quad (10.7)$$

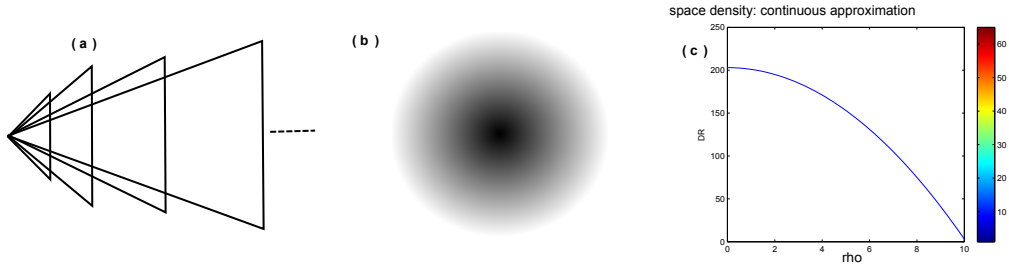


FIGURE 10.2: (a)  $n$  tetrahedra with a common corner. This illustrates the real case (three dimensional space); the triangles are replaced by tetrahedra and the 2d areas becomes 3d regions. (b) A visualization to the space density, around the gravity source, using color intensity. (c) A continuous approximation (analytic) to the space density as a function of  $\rho$ . The dashed line in (a) refers to additional structures which are not presented here.

where we have considered infinitesimal jumps with  $\delta j_R = \frac{1}{2}$ . Therefore, the number of regions along the  $R$ -line coordinate is  $n$ , i.e. we have  $\{R_j, j = \overline{1, n}\}$ . Accordingly to what we have done in the above example, it is clear that one can write:

$$\mathcal{D}_{R_i} = n + 1 - i = 2(j_R)_{\max} + 2 - i, \quad i = \overline{1, n}. \quad (10.8)$$

or as a function of  $\rho$  as

$$\mathcal{D}_R = 2(\eta - \rho^2) + 3. \quad (10.9)$$

where  $\eta = (j_R)_{\max}$  and  $\rho$  gets discrete values. Fig. ?? visualizes the structure. Note that restricting the computation of the space density to the contributions of the tetrahedra  $\{T_i, i = \overline{1, n}\}$  along the  $R$ -line coordinate is not just an abstract non physical example, it can be rigorously applied to test particles moving along geodesics, say , which belong to the  $R$ -line coordinate. It is to be noted that  $\{R_i, i = \overline{1, n}\}$  naturally include the change in the configurations of the tetrahedra. This is because of the fact that they are defined as intersections.

The very important results shown above open new trends and avenues for studying the properties of the spacetime structure. Exploring the properties already found concerning ordinary matter and the notion of density in the context of the present study will help to discover more the structure of spacetime.

## 10.2 Gravity as Mass Defect

Since the general theory of relativity papers have been published, the gravity theory still defined as a manifestation of curved geometry. Even quantitatively (e.g. loop gravity [1]), quantum geometries become arisen such as twisted and Regge geometries. But, the geometric aspect still the cornerstone.

More recently, the authors in Ref. [65] have shown that space is defined with a property called *space density*. In the present paper, we find that the space density property can interpret gravity very nicely. In fact, the space density found in Ref. 96 interpret gravity the same as mass defect, in nuclear physics, interprets the bending energy that holds nucleus together. This leads to state the main result the paper try to show: *gravity can be seen as mass defect happens to test particles.*

It is a well-known fact that the mass of a nucleus does not equal to the sum of its constituents masses. The difference called the *mass defect*. It serves as a binding energy holding the nucleus together. Surprisingly, something like this gets arisen in loop gravity. To see how does really work, let start with a simple example and then generalize the idea. We suppose (theoretically) that a test particle  $p$ , with mass  $m$  and volume  $V$ , is located in the tetrahedron  $T_3$  such that  $p_{\text{space}} \in R_3$  where  $p_{\text{space}}$  is defined by  $V = \int_{p_{\text{space}}} dx^3$ , that is the space occupied by the particle volume. Thus the volume mass  $\rho_p$  can be written as

$$m = \rho_p V = \int_{p_{\text{space}}} \rho_p dx^3 = \rho_p \int_{p_{\text{space}}} dx^3. \quad (10.10)$$

Now, how to define  $m$  when  $p_{\text{space}} \in R_2$  or  $\in R_1$ ?. We have seen that space is defined with density. Thus if we gauge the space density of separate tetrahedra (that is there are no intersections recorded on their regions) to be one, it is clear that  $\int_{p_{\text{space}}} dx^3$  for  $R_2$  and  $R_3$  must contain an additional term, say  $\mathcal{K}(\mathcal{D}_{R_i})$  where  $i = \overline{2,3}$ , referring to the density such that we have the map:

$$\pi_{3 \rightarrow i} : \int_{p_{\text{space}}} dx^3 \mapsto \int_{p_{\text{space}}} \mathcal{K}(\mathcal{D}_{R_i}) dx^3 = \mathcal{K}(\mathcal{D}_{R_i}) V \quad (10.11)$$

where the map practically refers to the jump of the test particle from  $R_3 \mapsto R_i$ ,  $i = 2, 3$ . Note that there is no clear arguments lead to identify the

quantity  $\mathcal{K}(\mathcal{D}_{R_i})$ . Thus we keep it unknown and symbolized by  $\mathcal{K}(\mathcal{D}_{R_i})$  until some evidence about get arisen. This because our understanding of the space structure is far from been practical and clear; its explicit definition may includes non trivial behavior. It is clear that in  $\pi_{3 \rightarrow i}$  the quantity of ordinary matter do not change (except the relativistic effect: increasing the mass with the velocity). This allows to answer the above question writing

$$m_{R_i} = \rho_p \int_{\text{Pspace}} \mathcal{K}(\mathcal{D}_{R_i}) dx^3 = \mathcal{K}(\mathcal{D}_{R_i}) \rho_p \int_{\text{Pspace}} dx^3 \quad (10.12)$$

where  $i = \overline{2, 3}$  and  $m_{R_i}$  is the test particle mass in  $R_2$  or in  $R_3$ . This leads to introduce a quantity called mass defect defined by the difference

$$\Delta m_i = m_{R_i} - m = (\mathcal{K}(\mathcal{D}_{R_i}) - 1)m. \quad (10.13)$$

But, what does this quantity serve for?. What we know, so far, about gravity is just the fact that gravity is a geometric theory based on the Einsteinien idea of curvature (except some new perspectives such as those in string theory which are not proved yet). The present novel quantity, mass defect, interprets very nicely the fact being gravitationally interacted. It simply states that when a test particle is moving in a gravitational field, it manifests a mass defect happens with it which becomes a *kinetic energy* (this should not be confused with the relativistic effects on the mass of the test particle which appears with the increase in the velocity). In fact, the mass defect found here has a very close notion to what it is well known as *gravitational potential energy*. Roughly, it replaces this notion.

It is to be noted that the novel quantity we have found, mass defect, it is not a strange and subtle result. In fact, the presence of this quantity can be traced back to the presence of the notion of space density (together with the fact that a test particle can not never be placed in a gravitational field without occupying a volume), which in turn can be traced back to the well-known fact in loop quantum gravity (more specifically the quantum polyhedron): the volume of space has the role of the Hamiltonian generating classical orbits, i.e. it has the role of energy which can be defined with a density.

Note that in the above study, we have considered a simple example. The general case (for a macroscopic motion) refers to the continuum where the

indice  $i$  is dropped and the density becomes  $\mathcal{D}_R$  (or more generally  $\mathcal{D}$  for a motion in the 3d space) , then the mass of a test particle depends on the position in the spacetime around the gravity source, which can be written generally as

$$m_{\text{phys}} = \mathcal{K}(\mathcal{D})m. \quad (10.14)$$

### 10.2.1 Gravity Force

How gravity force can be interpreted in the context of the present study?. Note that we have found a mass defect happens to test particles moving in a gravitational field. Together with the fact that the mass is equivalent to the energy (via Einstein relation  $E = mc^2$ ), the the gravity force becomes clear fact. More explicitly, we write (we have considered the jumps in the map  $\pi_{3 \rightarrow i}$  as presenting an infinitesimal motion, as it looks in the large scale)

$$dm = (\mathcal{K}(\mathcal{D}_{R_i}) - 1)m = \frac{dE}{c^2} = \frac{Fdx}{c^2} \quad (10.15)$$

where  $E$  the energy of the test particle,  $F$  the gravity force affecting it and  $dx = a$  the distance between the two tetrahedra in the jump (infinitesimal, as it looks in the large scale). The last relation leads to write

$$F = \frac{(\mathcal{K}(\mathcal{D}_{R_i}) - 1)mc^2}{a} \quad (10.16)$$

which gives the gravity force locally.

### 10.2.2 Gravitational Potential Energy

We have stated above that the mass defect replaces in fact the gravitational potential energy, how does really work?. It is a well known fact that test particles around a gravity source have potential energy. If we take a particle moving (near the earth surface) in the  $R$ -lined coordinates (radial motion) such that the distance  $a$  is the radial distance the particle moves. Thus, the particle will get a gravitational potential energy (when it moves from the source tetrahedron into the target one, separated by a distance  $a$ ) given by  $E_p = mga$  where  $g = 9.81$ . This energy manifests as a kinetic energy given by

$$E_c = \frac{1}{2}mv^2 = mga = (\mathcal{K}(\mathcal{D}_{R_i}) - 1)mc^2 \quad (10.17)$$



(we have supposed that the particle started with a zero velocity) where  $v$  its velocity at the target tetrahedron in the jump.

In summary, in this chapter, we find a new interpretation for the fact being gravitationally interacted. This very important result, although it is still a starting idea (not developed yet or generally accepted) for further development, open new trends in studying gravity and the quantum spacetime.

It is to be emphasized that there are no evidences, as much as we know, can be considered to identify the quantity  $\mathcal{K}(\mathcal{D})$ . Thus it still unidentified waiting future researches about.

# Chapter 11

## Conclusion

### 11.1 Summary of the Key Results

Loop gravity has brought and opened new trends and avenues in exploring the quantum structure of spacetime through its three well-known methods: canonical, covariant and geometrical approaches. In the semiclassical limit, the three approaches give close results. e.g. in Ref (28), it has been proved that the volume spectrum in the geometric approach has a good agreement with the spectrum found canonically in loop gravity. However in the deep quantum regime, each approach has its own behavior.

After the introductory chapters 1 and 2, we have seen that the  $SU(2)$  parametrization for loop gravity graph, as it has been proved this parametrization has a nice representation via the framework by Rovelli in Ref (11), can be interpreted in the more general case: twisted-truncation of general relativity. Then an explicit study on the exact nature of Schwarzschild Spacetime graph has been concluded and discussed. The study on the Schwarzschild Spacetime graph led us to find a new quantity called space density, which describe and provide a nice property for space like the one in ordinary matter. Next, we have found that Bohr-Sommerfeld quantization condition can be applied not only to the quantum tetrahedron but, more specifically, to the quantum trihedron. Moreover, the idea of virtual lines used in the canonical derivation of the volume of space has been proved that can be applied rigorously to derive the semiclassical spectrum of the volume. Then, we have seen that the quantum pentahedron behaves in a more analogous way to the behavior of ordinary matter at the quantum level: a representation on phase

spaces gives an atomic structure for the space structure closely related to the one in ordinary matter. Next, we have seen that the discreteness of the space measures, via Bohr-Sommerfeld quantization, is not only related to area and volume but even to the length of space quantization. The spectrum found matches well the one found in loop gravity.

## 11.2 Future Research Interests

- **Regge and Twisted Geometries in Loop Gravity:** The work done in this title concerns the euclidean case where the graph is constructed of  $N$  copies of  $SU(2)$ , the number of links constructing it. A future research will address the general case where the grains of space are four dimensional objects. The generalization is the step from an  $SU(2)$  parametrization of the loop gravity graph into  $SL(2, c)$  parametrization.
- **Regge and Twisted Geometries in Schwarzschild Spacetime:** The graph found and discussed in the title of this study open new trends and avenues in exploring the quantum structure of the Schwarzschild Spacetime. A future research will handle a numerical study for the Schwarzschild Spacetime geometry using the technical tools and the results found in the "Regge and Twisted Geometries in Schwarzschild Spacetime" paper.
- **Space Density from Loop Gravity:** the notion of space density open trends for studying the spacetime structure and its properties. A future works will address the the other solutions of Einstein's general theory of relativity equations.
- **Length of Space Quantization:** The main virtue in the length of space quantization shown in the paper of this title is that it considerably simplify the quantitative study of spacetime geometry. This because of the fact that all classical physics are based on the length of space description as a technical tool. The length of space quantization shown in the "the quantum tetrahedron and the length spectrum" paper handles the case of the quantum polyhedron. Future research will address the general case: the quantum polyhedron and the length spectrum.
- **The quantum Trihedron:** A followed work to the "The quantum Trihedron" paper will address the relation between the area of space

and the quantum polyhedron. An expected result is that the quantum polyhedron has structure analogous to the one of ordinary matter.

- **The Quantum Pentahedra:** In the "The Quantum Pentahedra" paper, an atomic structure of the quantum pentahedron has been discovered. The generalization of the work for the quantum polyhedron would give an analogous between the spacetime structure and ordinary matter. This work will be considered in a followed paper to the work.

# Appendix A

## The $SL(2, C)$ representations

Let start by giving the corresponding casimirs, which are

$$C_1 = \frac{1}{2} J_{IJ} J^{IJ} = k^2 - l^2 \quad (\text{A.1})$$

$$C_2 = \frac{1}{8} \epsilon_{ijkl} J^{IJ} J^{KL} = \vec{K} \cdot \vec{L}. \quad (\text{A.2})$$

In this derivation for  $|p, k, j, m\rangle$  of  $V^{(p,k)}$  one has to diagonalizes the corresponding operators. A direct computation allows to find the following (these were first derived and investigated by Gelfand et al (1963))

$$L^3 |j, m\rangle = m |j, m\rangle \quad (\text{A.3})$$

$$L^+ |j, m\rangle = \sqrt{(j+m+1)(j-m)} |j, m+1\rangle \quad (\text{A.4})$$

$$L^- |j, m\rangle = \sqrt{(j-m+1)(j+m)} |j, m-1\rangle \quad (\text{A.5})$$

$$k^3 |j, m\rangle = -\alpha_{(j)} \sqrt{j^2 - m^2} |j-1, m\rangle - \beta_{(j)} m |j, m\rangle + \alpha_{(j+1)} \Theta |j+1, m\rangle \quad (\text{A.6})$$

$$k^+ |j, m\rangle = -\alpha_{(j)} \varpi |j-1, m+1\rangle - \beta_{(j)} \vartheta |j, m+1\rangle - \alpha_{(j+1)} \varsigma |j+1, m+1\rangle \quad (\text{A.7})$$

$$k^- |j, m\rangle = \alpha_{(j)} \varpi |j-1, m-1\rangle - \beta_{(j)} \xi |j, m-1\rangle - \alpha_{(j+1)} \psi |j+1, m-1\rangle. \quad (\text{A.8})$$

where

$$\psi = \sqrt{(j-m+1)(j-m+2)} \quad (\text{A.9})$$

$$\xi = \sqrt{(j-m+1)(j+m)} \quad (\text{A.10})$$

$$\varsigma = \sqrt{(j+m+1)(j+m+2)} \quad (\text{A.11})$$

$$\vartheta = \sqrt{(j+m+1)(j-m)} \quad (\text{A.12})$$

$$\varpi = \sqrt{(j-m-1)(j-m)} \quad (\text{A.13})$$

$$L^\pm = L^1 \pm L^2 \quad (\text{A.14})$$

$$K^\pm = K^1 \pm K^2 \quad (\text{A.15})$$

$$\alpha_{(j)} = \frac{i}{j} \sqrt{\frac{(j^2 - k^2)(j^2 + p^2)}{4j^2 - 1}} \quad (\text{A.16})$$

$$\beta_{(j)} = \frac{pk}{j(j+1)}. \quad (\text{A.17})$$

$$\Theta = \sqrt{(j+1)^2 - m^2}. \quad (\text{A.18})$$

# Bibliography

- [1] Carlo Rovelli. *Quantum gravity*. Cambridge university press, 2007.
- [2] Carlo Rovelli and Francesca Vidotto. *Covariant Loop Quantum Gravity: An Elementary Introduction to Quantum Gravity and Spinfoam Theory*. Cambridge University Press, 2014.
- [3] Thomas Thiemann. Introduction to modern canonical quantum general relativity. *arXiv preprint gr-qc/0110034*, 2001.
- [4] Abhay Ashtekar. *Lectures on non-perturbative canonical gravity*, volume 4. World Scientific, 1991.
- [5] Carlo Rovelli and Lee Smolin. Discreteness of area and volume in quantum gravity. *Nuclear Physics B*, 442(3):593–619, 1995.
- [6] Alejandro Corichi. Comments on area spectra in loop quantum gravity. *arXiv preprint gr-qc/0402064*, 2004.
- [7] Laurent Freidel, Etera R Livine, and Carlo Rovelli. Spectra of length and area in  $(2+1)$  lorentzian loop quantum gravity. *Classical and Quantum Gravity*, 20(8):1463, 2003.
- [8] Anton Alekseev, AP Polychronakos, and Mikael Smedbäck. On area and entropy of a black hole. *Physics Letters B*, 574(3):296–300, 2003.
- [9] Alexios P Polychronakos. Area spectrum and quasinormal modes of black holes. *Physical Review D*, 69(4):044010, 2004.
- [10] G Gour and V Suneeta. Comparison of area spectra in loop quantum gravity. *Classical and Quantum Gravity*, 21(14):3405, 2004.
- [11] Simonetta Frittelli, Luis Lehner, and Carlo Rovelli. The complete spectrum of the area from recoupling theory in loop quantum gravity. *Classical and Quantum Gravity*, 13(11):2921, 1996.

- 
- [12] Ga'bor Helesfai and Gyula Bene. A numerical study of spectral properties of the area operator in loop quantum gravity. *arXiv preprint gr-qc/0306124*, 2003.
- [13] Johannes Brunnemann and David Rideout. Properties of the volume operator in loop quantum gravity: I. results. *Classical and Quantum Gravity*, 25(6):065001, 2008.
- [14] Johannes Brunnemann and Thomas Thiemann. Simplification of the spectral analysis of the volume operator in loop quantum gravity. *Classical and Quantum Gravity*, 23(4):1289, 2006.
- [15] You Ding and Carlo Rovelli. The volume operator in covariant quantum gravity. *Classical and Quantum Gravity*, 27(16):165003, 2010.
- [16] Gaspare Carbone, Mauro Carfora, and Annalisa Marzuoli. Quantum states of elementary three-geometry. *Classical and Quantum Gravity*, 19(14):3761, 2002.
- [17] Andrea Barbieri. Quantum tetrahedra and simplicial spin networks. *Nuclear Physics B*, 518(3):714–728, 1998.
- [18] John C Baez and John W Barrett. The quantum tetrahedron in 3 and 4 dimensions. *arXiv preprint gr-qc/9903060*, 1999.
- [19] John W Barrett and Louis Crane. Relativistic spin networks and quantum gravity. *Journal of Mathematical Physics*, 39(6):3296–3302, 1998.
- [20] Muxin Han. 4-dimensional spin-foam model with quantum lorentz group. *Journal of Mathematical Physics*, 52(7):072501, 2011.
- [21] John C Baez. Spin foam models. *Classical and Quantum Gravity*, 15(7):1827, 1998.
- [22] Jonathan Engle, Roberto Pereira, and Carlo Rovelli. Loop-quantum-gravity vertex amplitude. *Physical review letters*, 99(16):161301, 2007.
- [23] Jonathan Engle, Roberto Pereira, and Carlo Rovelli. Flipped spinfoam vertex and loop gravity. *Nuclear Physics B*, 798(1):251–290, 2008.
- [24] Jonathan Engle, Etera Livine, Roberto Pereira, and Carlo Rovelli. Lqg vertex with finite immirzi parameter. *Nuclear Physics B*, 799(1):136–149, 2008.



- 
- [25] Alejandro Perez. The spin foam approach to quantum gravity. *Living Rev. Rel*, 16(3):1205–2019, 2013.
- [26] Etera R Livine and Simone Speziale. New spinfoam vertex for quantum gravity. *Physical Review D*, 76(8):084028, 2007.
- [27] Eugenio Bianchi, Pietro Dona, and Simone Speziale. Polyhedra in loop quantum gravity. *Physical Review D*, 83(4):044035, 2011.
- [28] Eugenio Bianchi and Hal M Haggard. Discreteness of the volume of space from bohr-sommerfeld quantization. *Physical review letters*, 107(1):011301, 2011.
- [29] Eugenio Bianchi and Hal M Haggard. Bohr-sommerfeld quantization of space. *Physical Review D*, 86(12):124010, 2012.
- [30] John Schliemann. Classical and quantum polyhedra. *Physical Review D*, 90(12):124080, 2014.
- [31] Hal M Haggard, Muxin Han, and Aldo Riello. Encoding curved tetrahedra in face holonomies: Phase space of shapes from group-valued moment maps. In *Annales Henri Poincaré*, pages 1–48. Springer, 2015.
- [32] Eugenio Bianchi. Quantum geometry of space in spinfoam gravity. *Acta Physica Polonica B*, 44(12), 2013.
- [33] John Schliemann. The large-volume limit of a quantum tetrahedron is a quantum harmonic oscillator. *Classical and Quantum Gravity*, 30(23):235018, 2013.
- [34] CE Coleman-Smith and B Müller. A “helium atom” of space: Dynamical instability of the isochoric pentahedron. *Physical Review D*, 87(4):044047, 2013.
- [35] Ahmida Bendjoudi and Nouredine Mebarki. The quantum trihedron. *chinese physics letter*, 87(4):044047, 2013.
- [36] Abhay Ashtekar. New variables for classical and quantum gravity. *Physical Review Letters*, 57(18):2244, 1986.
- [37] J Fernando Barbero G. Real-polynomial formulation of general relativity in terms of connections. *Physical Review D*, 49(12):6935–6938, 1994.

- 
- [38] J Fernando Barbero G. Real ashtekar variables for lorentzian signature space-times. *Physical Review D*, 51(10):5507–5510, 1995.
- [39] Ted Jacobson and Lee Smolin. Nonperturbative quantum geometries. *Nuclear Physics B*, 299(2):295–345, 1988.
- [40] C Rovelli and L Smolin. A new approach to quantum gravity based on loop variables. In *International conference on Gravitation and Cosmology, Goa, Dec*, pages 14–19, 1988.
- [41] Abhay Ashtekar and Jerzy Lewandowski. Representation theory of analytic holonomy  $c^*$  algebras. *arXiv preprint gr-qc/9311010*, 1993.
- [42] Abhay Ashtekar and Jerzy Lewandowski. Differential geometry on the space of connections via graphs and projective limits. *Journal of Geometry and Physics*, 17(3):191–230, 1995.
- [43] Carlo Rovelli and Lee Smolin. Discreteness of area and volume in quantum gravity. *Nuclear Physics B*, 442(3):593–619, 1995.
- [44] Thomas Thiemann. Quantum spin dynamics (qsd). *Classical and Quantum Gravity*, 15(4):839, 1998.
- [45] Thomas Thiemann. Quantum spin dynamics (qsd): Ii. the kernel of the wheeler-dewitt constraint operator. *Classical and Quantum Gravity*, 15(4):875, 1998.
- [46] Thomas Thiemann. Anomaly-free formulation of non-perturbative, four-dimensional lorentzian quantum gravity. *Physics Letters B*, 380(3):257–264, 1996.
- [47] Carlo Rovelli. Outline of a generally covariant quantum field theory and a quantum theory of gravity. *Journal of Mathematical Physics*, 36(11):6529–6547, 1995.
- [48] Steven Carlip. Four-dimensional entropy from three-dimensional gravity. *Physical review letters*, 115(7):071302, 2015.
- [49] John W Barrett and Louis Crane. Relativistic spin networks and quantum gravity. *Journal of Mathematical Physics*, 39(6):3296–3302, 1998.
- [50] John C Baez. Spin foam models. *Classical and Quantum Gravity*, 15(7):1827, 1998.

- 
- [51] Andrea Barbieri. Quantum tetrahedra and simplicial spin networks. *Nuclear Physics B*, 518(3):714–728, 1998.
- [52] John C Baez and John W Barrett. The quantum tetrahedron in 3 and 4 dimensions. *arXiv preprint gr-qc/9903060*, 1999.
- [53] Laurent Freidel and Kirill Krasnov. A new spin foam model for 4d gravity. *Classical and Quantum Gravity*, 25(12):125018, 2008.
- [54] Benjamin Bahr, Frank Hellmann, Marcin Kisielowski, Jerzy Lewandowski, et al. Operator spin foam models. *Classical and quantum gravity*, 28(10):105003, 2011.
- [55] Thomas Thiemann. A length operator for canonical quantum gravity. *Journal of Mathematical Physics*, 39(6):3372–3392, 1998.
- [56] Eugenio Bianchi. The length operator in loop quantum gravity. *Nuclear physics B*, 807(3):591–624, 2009.
- [57] Yongge Ma, Chopin Soo, and Jinsong Yang. New length operator for loop quantum gravity. *Physical Review D*, 81(12):124026, 2010.
- [58] A. Bendjoudi and N. Mebarki. The quantum tetrahedron and the length spectrum. *has been accepted in IJMPD*, 2016.
- [59] A. Bendjoudi and N. Mebarki. The quantum trihedron. *has been accepted in CPL*, 2016.
- [60] A. Bendjoudi and N. Mebarki. Discreteness of the area of pace from ohr sommerfeld quantization. *submitted to EPL*, 2016.
- [61] A. Bendjoudi and N. Mebarki. The quantum polyhedron and the volume spectrum. *submitted to ijgmmp*, 2016.
- [62] A. Bendjoudi and N. Mebarki. The quantum pentahedron. *submitted to mpla*, 2016.
- [63] A. Bendjoudi and N. Mebarki. Regge and twisted geometries in loop gravity. *submitted to CPL*, 2016.
- [64] A. Bendjoudi and N. Mebarki. Regge and twisted geometries in schwarzschild spacetime. *submitted to IJMPD*, 2016.

- 
- [65] A. Bendjoudi and N. Mebarki. Space density from loop gravity. *in progress*, 2016.
- [66] Abhay Ashtekar. New variables for classical and quantum gravity. *Physical Review Letters*, 57(18):2244, 1986.
- [67] J Fernando Barbero G. Real ashtekar variables for lorentzian signature space-times. *Physical Review D*, 51(10):5507–5510, 1995.
- [68] Kirill V Krasnov. Geometrical entropy from loop quantum gravity. *Physical Review D*, 55(6):3505, 1997.
- [69] Kirill V Krasnov. On statistical mechanics of schwarzschild black hole. Technical report, SCAN-9705030, 1997.
- [70] Abhay Ashtekar and Jerzy Lewandowski. Quantum theory of geometry: I. area operators. *Classical and Quantum Gravity*, 14(1A):A55, 1997.
- [71] Abhay Ashtekar and Jerzy Lewandowski. Quantum theory of geometry ii: Volume operators. *arXiv preprint gr-qc/9711031*, 1997.
- [72] Jinsong Yang and Yongge Ma. New volume and inverse volume operators for loop quantum gravity. *arXiv preprint arXiv:1602.08688*, 2016.
- [73] Andrey Nikolayevich Tikhonov. On the stability of inverse problems. In *Dokl. Akad. Nauk SSSR*, volume 39, pages 195–198, 1943.
- [74] Seth A Major. Operators for quantized directions. *Classical and Quantum Gravity*, 16(12):3859, 1999.
- [75] Thomas Thiemann. Closed formula for the matrix elements of the volume operator in canonical quantum gravity. *Journal of Mathematical Physics*, 39(6):3347–3371, 1998.
- [76] Abhay Ashtekar and Jerzy Lewandowski. Quantum theory of geometry ii: Volume operators. *arXiv preprint gr-qc/9711031*, 1997.
- [77] H Minkowski. *Nachr. Ges. Wiss. Gottingen 198-219*, 1897.
- [78] Michael Kapovich, John Millson, et al. The symplectic geometry of polygons in euclidean space. *J. Differential Geom*, 44(3):479–513, 1996.

- [79] Jean B Lasserre. An analytical expression and an algorithm for the volume of a convex polyhedron in  $n$ . *Journal of optimization theory and applications*, 39(3):363–377, 1983.
- [80] Werner Heisenberg. Über quantentheoretische umdeutung kinematischer und mechanischer beziehungen. In *Original Scientific Papers Wissenschaftliche Originalarbeiten*, pages 382–396. Springer, 1985.
- [81] E Schrodinger. Quantisierung als eigenwertproblem,(dritte mitteilung: Störungstheorie, mit anwendung auf den strakeffekt der balmerlinien. *Ann. Phys.*, (4):474, 1926.
- [82] Max Born and Pascual Jordan. Zur quantenmechanik. *Zeitschrift für Physik*, 34(1):858–888, 1925.
- [83] Vincenzo Aquilanti, Hal M Haggard, Robert G Littlejohn, and Liang Yu. Semiclassical analysis of wigner 3j-symbol. *Journal of Physics A: Mathematical and Theoretical*, 40(21):5637, 2007.
- [84] Alexios P Polychronakos. Area spectrum and quasinormal modes of black holes. *Physical Review D*, 69(4):044010, 2004.
- [85] S Goshen, HJ Lipkin, F Bloch, SG Cohen, A de Shalit, S Sambursky, and I Talmi. Spectroscopic and group theoretical methods in physics, 1968.
- [86] Hal M Haggard. Pentahedral volume, chaos, and quantum gravity. *Physical Review D*, 87(4):044020, 2013.
- [87] Carlo Rovelli and Simone Speziale. Geometry of loop quantum gravity on a graph. *Physical Review D*, 82(4):044018, 2010.
- [88] Tullio Regge. General relativity without coordinates. *Il Nuovo Cimento (1955-1965)*, 19(3):558–571, 1961.
- [89] Laurent Freidel and Simone Speziale. Twisted geometries: a geometric parametrization of  $su(2)$  phase space. *Physical Review D*, 82(8):084040, 2010.
- [90] Laurent Freidel and Simone Speziale. Twistors to twisted geometries. *Physical Review D*, 82(8):084041, 2010.

- 
- [91] Shyang-Ling Lou and Yih-Shyan Su. Coherent spin-network states for loop quantum gravity in schwarzschild space-time. , (15):31–39, 2013.
- [92] Arundhati Dasgupta. Coherent states for black holes. *Journal of Cosmology and Astroparticle Physics*, 2003(08):004, 2003.
- [93] Luca Bombelli. Statistical geometry of random weave states. *arXiv preprint gr-qc/0101080*, 2001.

## DEVELOPPEMENT MATHEMATIQUE ET APPLICATIONS DE LA GRAVITATION QUANTIQUE A BOUCLES

Gravitation quantique à boucles est une théorie de principe pour décrire la structure quantique de spacetime à l'échelle de Planck, l'échelle à laquelle la relativité générale et la théorie quantique manifestent également. La théorie vient dans trois versions: L'approche canonique, approche covariante et approche géométrique. Toutes les approches utilisent le même espace de Hilbert, mais nous ne savons pas si elles correspondent en fait à la même théorie.

Dans cette thèse, je vais présenter nos principaux résultats dans la gravité quantique à boucles programme, qui se situent entre ces trois approches. Nous commençons par décrivant les approches canoniques et covariantes dans laquelle les notations et les concepts généraux de la théorie sont fixés. Ensuite, on calcule la longueur de l'espace, la longueur des arêtes tétraédriques. Après cela, nous étudions polyèdres quantique et sa relation avec la gravité quantique à boucles. Plus spécifique, nous discutons du tétraèdre quantique: le 4-noeud espace de Hilbert. Nous terminons le chapitre en examinant notre contribution dans les quantum polyèdres: la discrétisation de l'espace en utilisant Bohr-Sommerfeld quantification. Dans le suivant, nous dériverons le volume d'espace pour nombre arbitraire de faces du polyèdre. Nous utilisons le idée de lignes virtuelles ainsi que le fait que le noeud espace de Hilbert avec valences  $N$  peut être cracher en série de connectés 4-valences nœuds espaces de Hilbert. Ensuite, nous étudions la pentaèdre quantique dans lequel une belle représentation sur les espaces de phase pour les atomes pentaèdres d'espace est donné. Ensuite, nous étudions: (a) Regge et Twisted Géométries dans le contexte de la Gravity à boucle et (b) Regge et Twisted Geometries dans Schwarzschild Spacetime. En plus, le graphique de Schwarzschild Spacetime est bien étudiée. Enfin, une nouvelle quantité appelé densité d'espace est introduit et une interprétation de la force de gravité est discuté.

### Mots-clés:

gravitation quantique à boucles; Spin Foam; Méthodes semiclassique; La gravité quantique

## MATHEMATICAL DEVELOPMENT AND APPLICATIONS OF LOOP QUANTUM GRAVITY

Loop Quantum gravity is a tentative theory to describe the quantum structure of spacetime at the Planck scale, the scale at which both general relativity and quantum theory manifest equally. The theory comes in three versions: The canonical approach, covariant approach and geometric approach. All the approaches use the same Hilbert space, but we do not know whether they actually correspond to the same theory.

In this thesis, I will present our main results in the loop quantum gravity program, all of which lie in between the three approaches. We start with describing The canonical and covariant approaches in which the notations and general concepts of the theory are fixed. Then, we discuss our contribution on the length spectrum of space, the length of the tetrahedral edges. After that, we investigate the quantum polyhedra and its relation to loop quantum gravity. More specifically, we discuss the quantum tetrahedron: the 4-node Hilbert space. We finish the chapter by investigating our contribution in the field the quantum polyhedra: the discreteness of the area of space via Bohr-Sommerfeld quantization. Next, we investigate our deriving to the volume of space spectrum for arbitrary number of faces of the polyhedron. We use the idea of virtual lines together with the fact that the node Hilbert space with valency  $N$  can be split into series of connected 4-valent nodes Hilbert spaces. Then, we study the quantum pentahedron in which a nice representation on phase spaces for the pentahedral atoms of space is given. Next, we investigate our works on: (a) Regge and Twisted Geometries in the context of the loop Gravity Hilbert space and (b) Regge and Twisted Geometries in Schwarzschild Spacetime. We discuss the interesting results in which twisted-truncation is included in interpreting the loop gravity graph. Furthermore, the Schwarzschild Spacetime graph is well-studied. Finally, a new quantity called space density is introduced and an interpretation for gravity force is discussed.

**Key Words:** Loop Quantum Gravity; Spinfoam; Semiclassical Methods; Quantum gravity